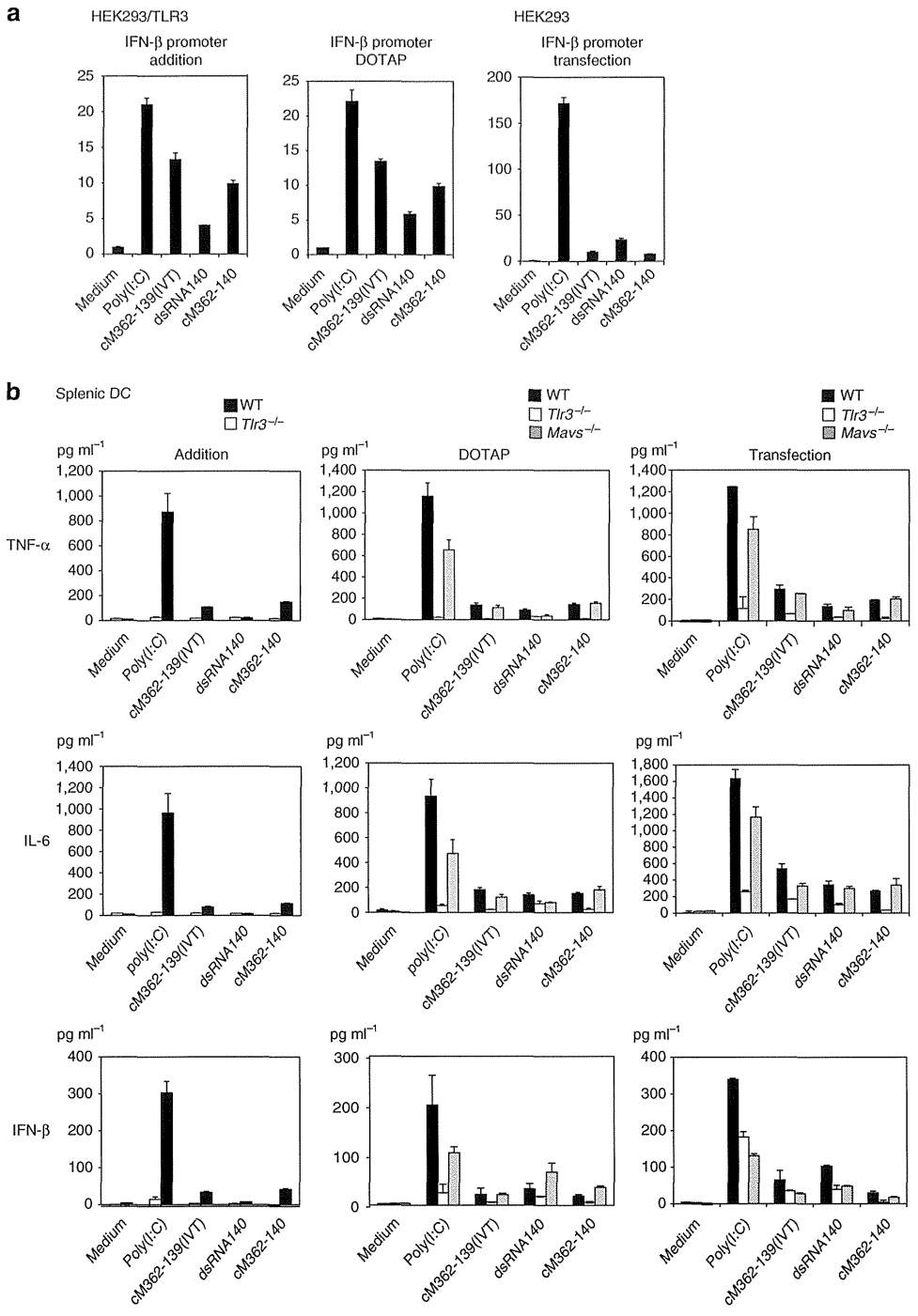

Figure 2 | TLR3-activating ability of cM362-140 in human and mouse cells. (**a**) TLR3-dependent IFN-β promoter activation by cM362-140. HEK293 cells were transiently transfected with IFN-β reporter and phRL-TK together with (left and middle panels) or without the expression plasmid for hTLR3 (right panel). Twenty-four hours after transfection, culture medium was removed and 10 μg ml^{-1} poly(I:C), cM362-139(IVT), dsRNA140 or cM362-140 in fresh medium (left panel), or the same compounds complexed with DOTAP liposomal reagent (middle panel), or with Lipofectamine 2000 (right panel) were added to cells. Luciferase activity was measured 6 h (left and middle panel) or 24 h (right panel) after stimulation, and expressed as fold induction relative to the activity of non-stimulated cells. Representative data from three independent experiments, each performed in triplicate, are shown (mean ± s.d.). (**b**) Splenic CD11c^{+} DCs (1.0×10^{6} per ml) isolated from *Tlr3*$^{-/-}$, *Mavs*$^{-/-}$ or WT mice were stimulated with 10 μg ml^{-1} untreated (left panels), DOTAP liposomal reagent-conjugated (middle panels) or Lipofectamine 2000-conjugated (right panel) nucleic acids as indicated. Twenty-four hours after stimulation, IFN-β in the culture supernatants was quantified using ELISA. TNF-α and IL-6 levels were measured using CBA. Representative data from three to five independent experiments are shown (mean ± s.d.).

treatment with cM362-140 caused barely any regression of EG7 tumours in this model (Fig. 5a). Nevertheless, combination therapy with OVA + cM362-140 still induced tumour growth retardation (Fig. 5a). OVA-specific CD8^{+} T cells proliferated and activated in the mice stimulated with OVA + cM362-140, as assessed by tetramer assay (Fig. 5b) and IFN-γ production (Fig. 5c). We confirmed that the induction of OVA-specific CD8^{+} T-cell activation by cM362-140 + OVA largely depends

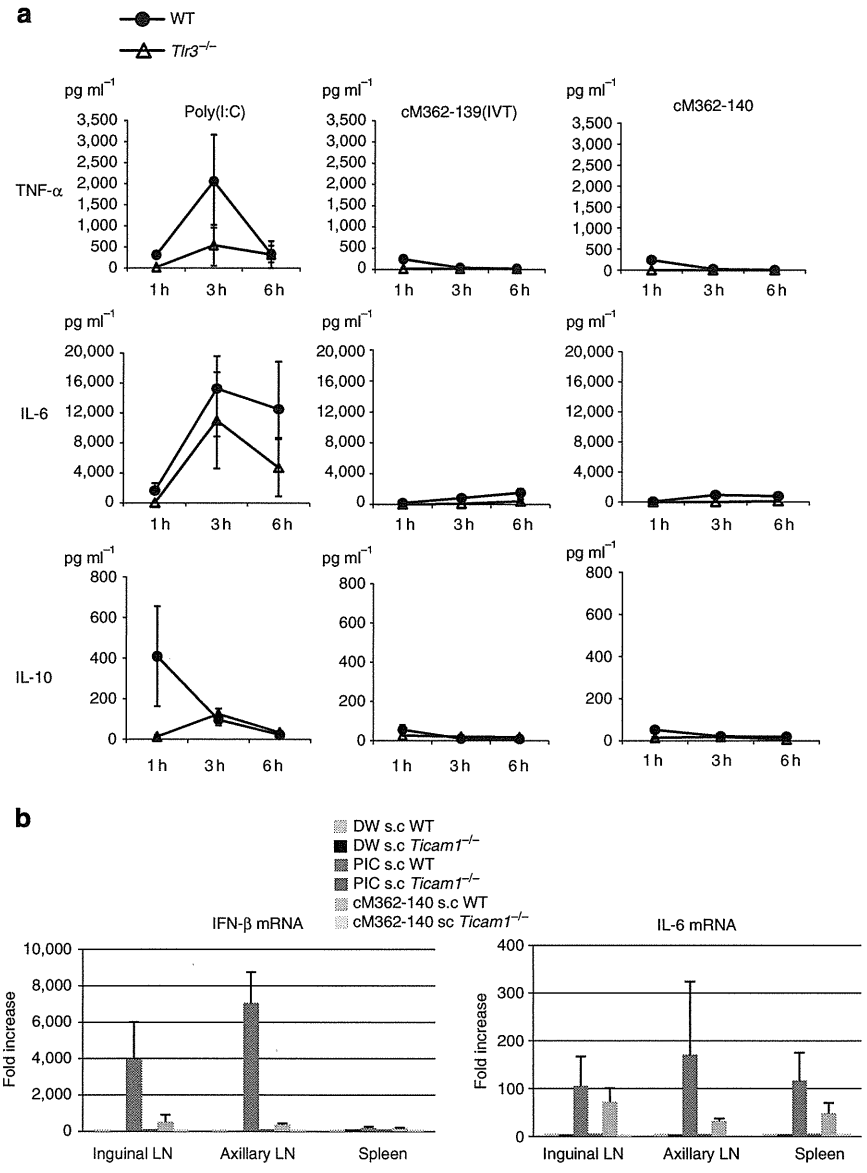

Figure 3 | cM362-139(IVT) and cM362-140 do not induce inflammatory cytokines. (**a**) Wild-type or *Tlr3*$^{-/-}$ female mice (9 week) were injected i.p. with 50 μg poly(I:C), cM362-139(IVT) or cM362-140 in RNase-free water. At timed intervals, blood was collected from the tail vein and TNF-α, IL-6 and IL-10 levels in each sample were measured using a CBA. Data are shown as the mean ± s.e.; $n=3$ mice per group. (**b**) Wild-type or *Ticam*$^{-/-}$ female mice were injected s.c. with distilled water (DW), poly(I:C) or cM362-140 in RNase-free water. After 6 h, spleen, inguinal and axillary LNs were harvested and *IFN-β* and *IL-6* mRNA expressions were quantified by qPCR. Data are expressed as the fold induction relative to the expression in DW-injected mice and shown as the mean ± s.e.; $n=3$ mice per group.

on TLR3/TICAM-1 using KO mice (Supplementary Fig. 9). Although polyI:C induces RIP1/3-mediated necroptosis via TICAM-1 in some tumour lines, cM362-140 was not the case in EG7 tumour (Supplementary Fig. 10). Hence, TLR3 has an important role in inducing cM362-140-mediated immune response and tumour growth retardation in the s.c. setting we employed in this study.

Antigen-specific CD8$^+$ T-cell priming by cM362-139/140. The Ag-specific CD8$^+$ T-cell priming ability of cM362-139/140 in tumour-free settings was next examined using spleen and inguinal LN cells. Wild-type mice were injected s.c. with OVA with or without RNA adjuvants twice per week. Since OVA-specific CD8$^+$ T cells most proliferated in spleen or inguinal LN 4 days after the last injection of OVA + poly(I:C) (Fig. 6a), spleen and LN cells were harvested from mice 4 days after the last adjuvant injection. cM362-139/140 significantly induced OVA-specific CD8$^+$ T-cell proliferation in the inguinal LN and spleen compared with poly(I:C) (Fig. 6b). OVA-specific IFN-γ production in spleen cells was also efficiently induced by cM362-139(IVT) and cM362-140 (Fig. 6c). The TICAM-1 pathway was mainly involved in Ag-specific CD8$^+$ T-cell activation induced by cM362-140 (Fig. 6d).

NK cell-mediated B16 tumour regression by cM362-139/140. Using a C57BL/6-B16 syngeneic NK-sensitive tumour-implant model[9], we evaluated NK-dependent antitumour activity of cM362-139(IVT) injected s.c. around the pre-formed tumour (Fig. 7a). Suppression of tumour growth, determined as reported previously[9], was observed in the group that received cM362-139(IVT) compared with the water-treated group. The retardation of B16 tumour growth appeared to depend on TLR3

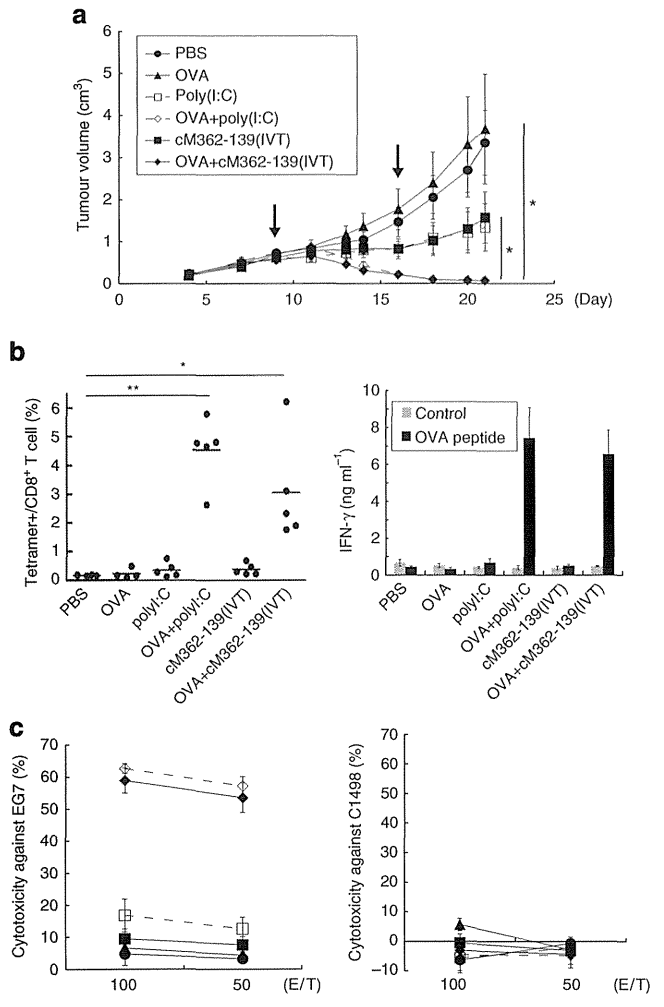

Figure 4 | cM362-139(IVT) induces CTL-mediated tumour regression. (**a**) Antitumour effect of cM362-139(IVT). WT mice were challenged with EG7 cells, and 7 and 14 days later they were s.c. injected with control PBS (●), OVA (▲), polyI:C (□) and OVA + polyI:C (◇) or cM362-139(IVT) (■) or OVA + cM362-139 (◆). Tumour size was evaluated in each group. All error bars used in this figure show ± s.e.m. Data are representative of two independent experiments. Each group consisted of five mice. *$P<0.05$ (ANOVA with Bonferroni's test). (**b**) OVA-specific CTL induction by cM362-139(IVT). Left panel: spleen cells were harvested at day 21 (7 days after 2nd therapy) and the proportion of tetramer-positive cells/CD8+ T cells was evaluated. *$P<0.05$, **$P<0.01$. Right panel: spleen cells were harvested at day 21 as for the left panel. The cells were stimulated with OVA peptide for 3 days and the level of IFN-γ in the culture supernatant was measured. (**c**) Ag-specific cytotoxicity induced by cM362-139(IVT). Splenocytes collected from tumour-bearing mice at day 21 were cultured in the presence of immorbilized EG7 for 5 days. Then, the cytotoxicity against EG7 (left panel) or C1498 (control, right panel) was measured by ^{51}Cr release assay.

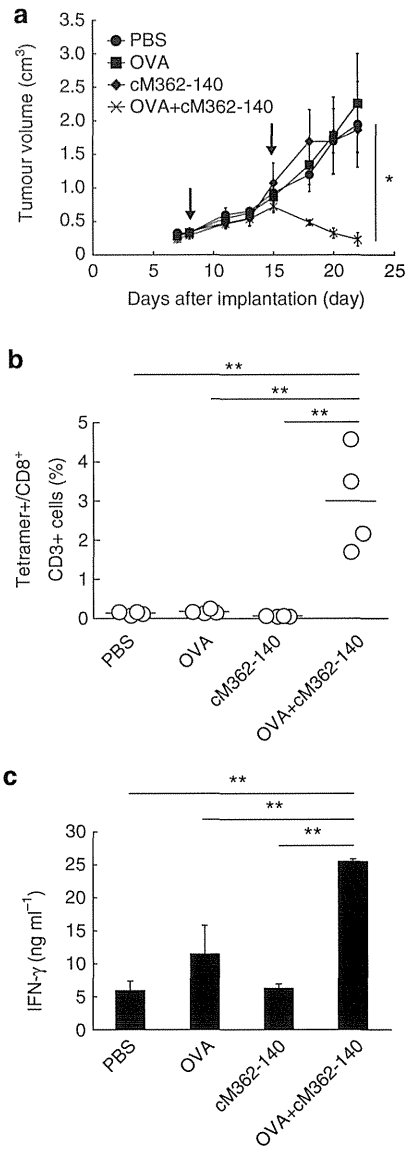

Figure 5 | cM362-140 induces EG7 tumour growth retardation. (**a**) Antitumour effect of cM362-140. As in Fig. 4, tumour-bearing mice were s.c. injected with PBS, OVA, cM362-140 and OVA + cM362-140 at timed intervals (days 8 and 15). Tumour size was evaluated in each group. (**b**) OVA-specific CTL induction by cM362-140. The proportion of tetramer-positive cells/CD8+ T cells in spleen was evaluated at day 22 (7 days after 2nd therapy). (**c**) Ag-specific IFN-γ production induced by cM362-140. Splenocytes were harvested at day 22 and incubated with OVA peptides for 3 days. The level of IFN-γ in the supernatant was measured by ELISA. *$P<0.05$, **$P<0.01$ (ANOVA with Bonferroni's test).

and TICAM-1 (Fig. 7a,b). NK1.1+ cells were involved in this tumour growth retardation (Fig. 7c), consistent with the NK-sensitive properties of B16 cells. No direct tumour cytolysis by macrophages[31] was associated with B16 growth retardation in the cM362-139(IVT) therapy. Splenocytes from the cM362-139(IVT)-treated group exerted higher cytotoxicity than those from the control group *in vitro* (Fig. 7d).

The chemically synthesized TLR3 ligand cM362-140 expressed a similar tumour-suppressing activity against B16 implant melanoma in the same model (Fig. 7e). This cM362-140-mediated NK-tumoricidal activity on B16 tumours was abrogated in *Ticam1*$^{-/-}$ mice (Fig. 7e). Thus, cM362-140 suppresses NK-sensitive tumours *in vivo* via TLR3 by acting as an NK-inducing adjuvant.

Discussion

Cancer immunotherapy relies on suitable adjuvants. Many TAA peptides have been synthesized, but the lack of an appropriate adjuvant to induce an immune response against the peptides has hampered progress in peptide vaccine therapy. Although many candidates, most of which were retrospectively recognized as TLR

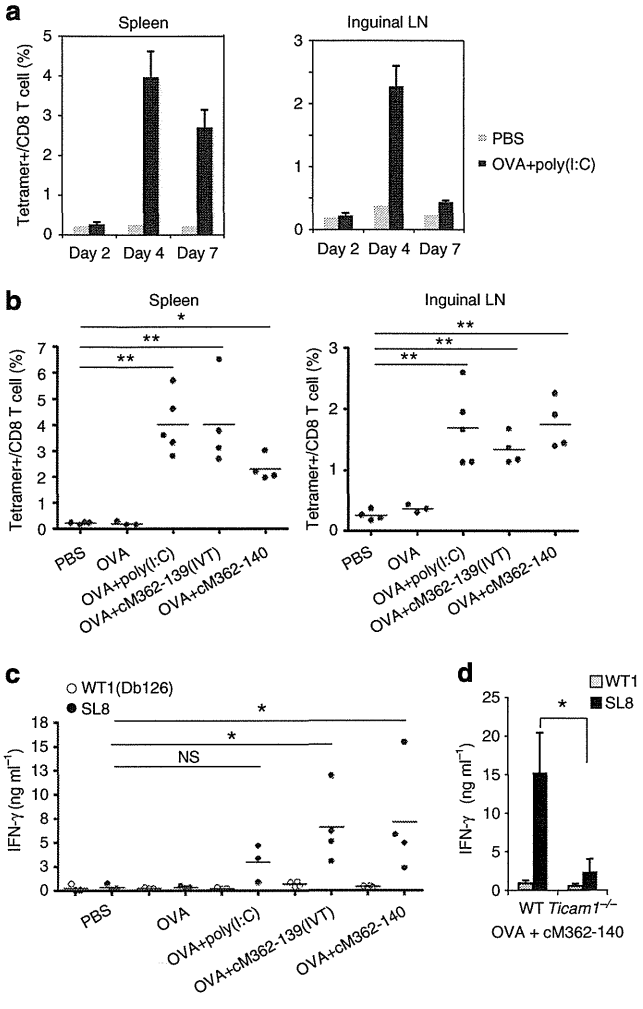

Figure 6 | cM362-139/140-induced antigen-specific CD8 T-cell activation in tumour-free settings. (**a**) Time-course experiments of poly(I:C)-induced antigen-specific CD8 T-cell activation in spleen and inguinal LN. WT mice were injected s.c. with 100 μl PBS or 50 μg poly(I:C) + 100 ng OVA twice per week. Spleen and inguinal LN cells were harvested at 2, 4 or 7 days after the last adjuvant injection and an increase of OVA-specific CD8 T-cell proliferation was evaluated with tetramer assay. (**b**,**c**) WT mice were injected s.c. with PBS, OVA, OVA + 50 μg poly(I:C), OVA + 50 μg cM362-139(IVT) or OVA + 70 μg cM362-140 twice per week. Spleen and inguinal LN cells were harvested 4 days after the last adjuvant injection and an increase of OVA-specific CD8 T-cell proliferation (**b**) and IFN-γ production (**c**) were then evaluated. (**b**) Proportion of tetramer-positive cells/CD8 T cells in spleen and inguinal LN. (**c**) Spleen cells were stimulated with OVA (SL8) or WT1 (Db126) peptide for 3 days and the level of IFN-γ in the culture supernatant was measured using a CBA. NS, no significant (>0.05), $*P<0.05$, $**P<0.01$, compared with PBS control (ANOVA with Dunnett's test). (**d**) cM362-140 + OVA induced Ag-specific CTL activation via the TICAM-1 pathway. Wild-type or *Ticam1*$^{-/-}$ mice were injected s.c. with PBS, OVA or OVA + cM362-140 as described above. Spleen cells were harvested 4 days after the last adjuvant injection and OVA-specific IFN-γ productions were assessed. PBS or OVA injection did not induce IFN-γ production from spleen cells. The data from OVA + cM362-140 injection are shown. $*P<0.05$ (Student's *t*-test).

agonists, have been tested in humans[1,6], they have not yet been clinically approved because of their undesired effects.

In this study, we designed many nucleotide adjuvants and tested their functional properties. Our approach is timely since most dsRNA receptors have been identified in the mouse and

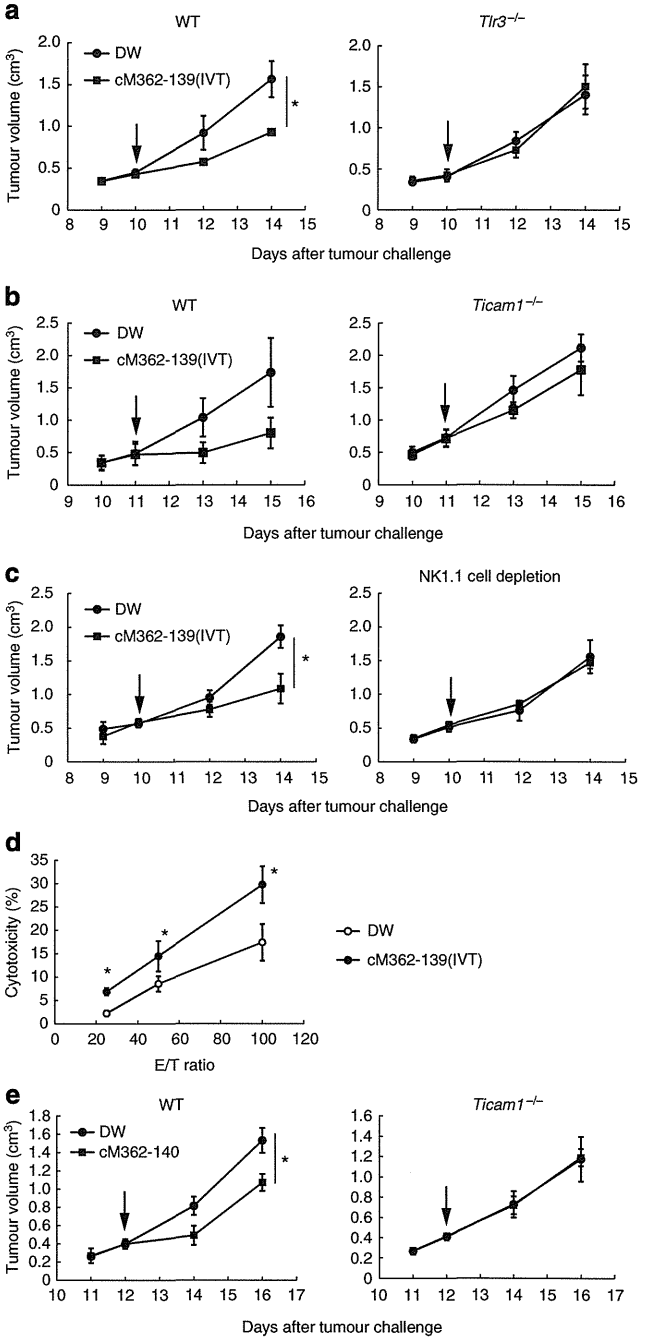

Figure 7 | Therapeutic effects of sODN-dsRNA in B16 tumour-implant model. (**a**,**b**) B16 tumour growth in mice after cM362-139(IVT) treatment. B16 melanoma cells were s.c. implanted into B6 WT mice (**a** and **b**), *Tlr3*$^{-/-}$ mice (**a**), or *Ticam1*$^{-/-}$ mice (**b**). cM362-139(IVT) or distilled water was injected s.c. around the tumour on the day indicated by arrow and then tumour volume was measured. Data are shown as tumour average volume ± s.e.; $n=3$ mice per group. $*P<0.05$. (**c**) Effect of NK cell depletion on cM362-139(IVT) treatment. Tumour-bearing mice were injected with anti-NK1.1 antibody to deplete NK cells. After 24 h, cM362-139(IVT) or distilled water was injected into the mice as described in **a**. (**d**) Cytotoxic activity of DX5$^+$ NK cells isolated from cM362-139(IVT)-treated mice. DX5$^+$ cells were isolated from B16 tumour-bearing mice treated with cM362-139(IVT) or distilled water for 18 h. Cytotoxic activity of DX5$^+$ cells against B16 target cells was measured by ^{51}Cr release assay. (**e**) B16 tumour growth in mice after cM362-140 treatment. Tumour-bearing mice were treated with cM362-140 as described in **a**.

human[1–4], and their structures and properties have been known for a decade[32–34]. Based on our current understanding of the dsRNA response, poly(I:C) activates both TICAM-1 (ref. 35) and MAVS pathways[36] resulting in systemic cytokinemia in mice[21,37]. Viral replication intermediates, double-stranded RNA and 5′-triphosphate RNA cause activation of the RLR pathway and robust cytokine production[38,39]. Here we chemically synthesized and tested a synthetic compound, cM362-140, an sODN-dsRNA that entered the endosomes and activated the TLR3/TICAM-1 pathway *in vivo*. Specifically, cM362-140 activated TLR3 in myeloid cells, including DCs in draining LNs, and induced activation of NK cells and proliferation of CTL. There was no systemically significant production of cytokines, including IFNs, after treatment with cM362-140. Our study establishes the proof-of-concept that modified or complexed RNA can regulate the immune response through TLR3 (refs 37,40), and that cM362-140 performs this function *in vivo*.

In this study, a systemic increase in the cytokine levels was not required for the induction of an antitumour immune response. Instead, a basal cytokine level effectively primed DCs to activate tumoricidal NK cells and CTL response. Subcutaneous or i.p. injection of cM362-140 barely activated the RLR pathway, whereas poly(I:C) activated this pathway to induce systemic cytokinemia. cM362-140 activated TICAM-1 for DC maturation, but barely induced chemokine production or necroptosis in tumour cells (Supplementary Fig. 10), which were reported as a direct action of poly(I:C)[29,30]. Therefore, cM362-140 eliminates major inflammatory responses caused by poly(I:C).

The 5′-sODN sequence of cM362-140 targeted the dsRNA to the endosome and evaded recognition by RIG-I/MDA5. A 140-bp stretch of dsRNA was required for TLR3 multimerization and TICAM-1 activation, but unsatisfactory for endosome targeting[40,41]. The 5′-sODN sequence of cM362 does not contain a CpG motif, which stimulates cytokine production via TLR9 in plasmacytoid DC. To prevent Dicer-mediated RNA interference, RNA sequences specific to human mRNAs were not employed. In addition, the antisense 5′-end of cM362-140 was OH, neither phosphorylated nor capped, unlike viral or host RNA products. Although cM362-140 was an artificial compound to circumvent host innate sensors, its constituents are native and modifiable to maximize antitumour response. Although the nucleic acid-sensing system differs somewhat between mouse and human[2,4]: generally, human BDCA3$^+$ DCs express a high level of TLR3 but no TLR9 (ref. 20), whereas mouse CD8α^+ DCs express TLR3 and TLR9 (refs 2,18,41), extrapolating results from the mouse and applying them to the human will be crucial for establishing human immunotherapy in the future.

Type I IFNs have remarkable antiviral and antitumour properties, but sometimes elicit severe side effects during treatment in patients. For example, s.c. injection of poly(I:C) induces inflammation, erythema and fever[42]. In clinical trials, cancer patients cannot tolerate high doses of poly(I:C), even if administered via s.c. injection[11,42–44]. Poly(I:C) consists of polyI and polyC chains of variable lengths that differ in function from one batch to the next, and, for unknown reasons, exogenous poly(I:C) activates cytoplasmic RNA sensors[36]. By contrast, cM362-140 is uniform. It binds TLR3 and fails to activate cytoplasmic RNA sensors, indicating that immune modulation by RNA occurs only in the draining LNs and tumour microenvironment[45]. Thus, cM362-140 enables us with a 'defined' immunotherapy to patients without systemic cytokine response or inflammation.

Several compounds that activate the TICAM-1 pathway are clinically available. Monophosphoryl lipid A is a TLR4 adjuvant that activates the TICAM-2/TICAM-1 cascade via TLR4/MD-2 (ref. 46). However, monophosphoryl lipid A still retains the TLR4-mediated MyD88 activation, which conceptually different from sODN-dsRNA that activates a single cascade of PRR. Although poly(A:U) mildly activates the TLR3 pathway and induces type I IFN in humans[47], it has far less adjuvancy than poly(I:C)[6,28,48]. In a short-term clinical trial, poly(I:C$_{12}$U), also known as ampligen, has been shown to be less toxic than other immunotherapies[49,50]. Unfortunately, data on its uniformity and TLR3-specificity as an adjuvant are scant. Poly(I:C)LC, another antitumour adjuvant, has shown clinical promise, but it causes cytokine toxicity, thereby precluding its further development[5,6,42–44,51]. Type I IFN induction and the output of IFNAR activation appear to be predominant in low-dose poly(I:C) administration in human volunteers[42]. In another clinical study, a low dose (1.4 mg per body) of poly(I:C)LC in combination with NY-Eso-1, which contains TAA epitopes, has been shown to mount a tumour-specific T-cell response[11]. Although low doses of poly(I:C)LC induce type I IFN, it only insufficiently stimulates T-cell proliferation *in vivo*[11]. cM362-140 is advantageous over poly(I:C)LC in that a high dose can be used to specifically activate TICAM-1, but not MAVS *in vivo*. This is the first report of the successful chemical creation of a long, sequence-defined and bioactive TLR3-specific ligand.

The targeting of programmed cell death-1 and cytotoxic T-lymphocyte-associated protein-4 with monoclonal antibodies in patients with progressive-staged cancer may provide another immunotherapy breakthrough[52]. Except for an alum adjuvant that can induce a Th2 response[2,53], there is no suitable adjuvant-TAA combination for immunotherapy. Immune enhancing by adjuvant would be required since tumour cells can undergo mutations and survive to circumvent immune attack. A main problem is that current adjuvant candidates are all inflammatory, facilitating formation of tumour-supporting microenvironment, that accelerates genome instability, tumour growth and progression[45]. Here, sODN-dsRNA is a non-inflammatory adjuvant sustaining DC-mediated NK/CTL activation, its combining with TAAs will bring a therapeutic benefit to a number of patients with intractable tumours.

Methods

Cell culture, reagents and plasmid. HEK293 cells were maintained in Dulbecco's Modified Eagle's medium (Invitrogen) supplemented with 10% heat-inactivated FCS (Invitrogen) and antibiotics. HeLa cells were kindly provided by Dr T. Fujita (Kyoto University) and maintained in Eagle's minimal essential medium (Nissui,) supplemented with 1% L-glutamine and 5% FCS. B16D8 melanoma cells were cultured at 37 °C under 5% CO_2 in RPMI containing 10% FCS, penicillin and streptomycin. EG7 and C1498 cells were purchased from ATCC and cultured in RPMI-1640 supplemented with 10% FCS, 55 μM 2-mercaptoethanol (2-ME) and 1 mM sodium pyruvate, and RPMI-1640 supplemented with 10% FCS and 25 ng ml^{-1} 2-ME, respectively. Poly(I:C) was purchased from Amersham Biosciences. Endotoxin-free ovalbumin was purchased from Hyglos. $OVA_{257-264}$ peptide (SL8), control WT1 peptide (Db126) and OVA ($H2K^b$-SL8) tetramer were from MBL. Human serum type AB was from Lonza. ODNs were synthesized by GeneDesign. Following antibodies were used in this study: Alexa Fluor-568-conjugated secondary antibody (Invitrogen), FITC-CD8α (53-6.7) and APC-CD3ε (145-2C11) (BioLegend), and PerCP/Cy5.5-7AAD (BD Biosciences). The human TLR3 expression plasmid was constructed in our laboratory[33].

Preparation of *in vitro* transcribed sODN-dsRNAs. The leader-trailer sequence of a MV laboratory-adapted strain of Edmonston was used as the dsRNA template[25]. DNA fragments covering this region of the MV genome and the T7 promoter sequence were amplified using PCR with specific primers and the plasmid pCR-T7 MV as a template. Sense and antisense MV RNAs from the PCR products were *in vitro* transcribed using an AmpliScribe T7 transcription kit (Epicentre Technologies) according to the manufacturer's protocol. The transcribed products were purified by 8% PAGE containing 7 M urea. After visualization by ultraviolet illumination, the appropriate bands were excised and eluted with 0.3 M sodium acetate. The eluted RNAs were ethanol precipitated and resuspended in RNase-free water. For large-scale preparation of RNAs, electro-elutions were performed using D-Tube Dialyzer Maxi (Novagen) and eluted RNAs were dialyzed, concentrated and precipitated with ethanol. The concentration of RNA was determined by measuring the absorbance at 260 nm in a

spectrophotometer. To generate sODN-dsRNA, sODN + linker DNA, sense and antisense RNA were mixed and annealed. sODNs, MV RNA sequences in sODN-dsRNA and PCR primers used in this study are described in Supplementary Tables 1–3.

Preparation of cM362-140. The chemically synthesized long RNAs as an alternative to *in vitro* transcribed RNAs were completed by a ligation reaction mediated by splint DNA[54] with slight modification. The outline of chemical synthesis was described below.

To prepare the sense strand of cM362-140, the ligation reactions were performed in two steps. First, S2 RNA (40 nmol), S3 RNA (40 nmol) and specific splint DNA (40–48 nmol) were mixed, heated at 90 °C for 5 min and slowly cooled to 4 °C (Supplementary Table 4A,B). Following hybridization, T4 DNA ligase (Takara) was added and incubated at room temperature for 16–22 h. The ligation reaction mixtures comprised 15.4 μM annealed complex, 66 mM Tris-HCl (pH 7.6), 6.6 mM $MgCl_2$, 10 mM DTT, 0.1 mM ATP and ~31 U μl^{-1} T4 DNA ligase. As the second ligation, S1 cM362-RNA (40 nmol) and the specific splint DNA (40–48 nmol) for the second ligation site were added into the first ligation reaction mixture, hybridized and T4 DNA ligase was added. The mixture was incubated at room temperature for 16–22 h. The derived full-length 165 mer sense strand was isolated by 8% PAGE containing 7 M urea and electro-elution. The subsequent procedure was the same as described in the section describing purification of *in vitro* transcribed RNAs. Overall yield was 8–10%.

To prepare the antisense RNA of cM362-140, three fragment RNAs, AS1, AS2 and AS3 (33 nmol each) and the related splint DNAs (33 nmol each) were mixed, hybridized and then T4 DNA ligase was added. The mixture was incubated at room temperature for 16–22 h. The following procedure was the same as described above. Overall yield was 15–22%. To generate cM362-140, sense- and antisense-RNAs were annealed.

Analysis with microchip electrophoresis. To analyse the cM362-139 complex, we used a microchip electrophoresis instrument (model SV1210; Hitachi Electronics Engineering Co. Ltd.). The standard procedure for electrophoresis using 2-mercaptoethanol (ME) has been previously described[55,56]. sODN or RNAs were adjusted to 0.2 μM with water. The sODN/RNA1/RNA2 complex (designated cM362-139) and dsRNA (RNA1 + RNA2) were prepared by mixing DNA or RNAs and hybridizing in water (final concentration 0.4 μM). The sample solution (10 μl) was applied to the sample well of the microchip device and the programme was run at 600 V for 120 s (injection time), then at 1,100 V for 180 s (separation time) under 350 V of return voltage at 20 °C. During the electric separation, DNA or RNA peaks were detected by laser induced fluorescence and analysed.

Agarose gel electrophoresis. cM362-139(IVT) and cM362-140 were incubated in PBS or in RNase-free water with or without serum, for 60 min at 37 °C or 42 °C. Aliquots containing 0.1–0.2 μg of incubated sODN-dsRNAs were then mixed with 10 × loading dye (Takara Bio Inc.) and loaded onto 3 or 4% agarose gel (Nusieve 3:1 Agarose, Lonza) containing ethidium bromide. After electric separation, nucleic complexes were visualized using ultraviolet transilluminator (FAS-III, Toyobo).

Reporter gene assay. HEK293 cells (8×10^5 cells per well) were cultured in six-well plates and transfected with the TLR3 expression vector or empty vector (400 ng per well) together with the reporter plasmid (400 ng per well) and an internal control vector, phRL-TK (Promega; 20 ng per well) using Lipofectamine 2000 (Invitrogen). The p-125 luc reporter containing the human IFN-β promoter region (−125 to +19) was provided by Dr T. Taniguchi (University of Tokyo). Twenty-four hours after transfection, cells were collected and resusupended in medium with or without FCS. Then, cells were seeded into 96-well plates and stimulated with the indicated RNAs for 6 h. The *Firefly* and *Renilla* luciferase activities were determined using a dual-luciferase reporter assay kit (Promega). The *Firefly* luciferase activity was normalized to the *Renilla* luciferase activity and was expressed as the fold induction relative to the activity in unstimulated vector-transfected cells. All assays were performed in triplicate.

Cytokine assay. Splenic $CD11c^+$ DCs from wild-type, $Tlr3^{-/-}$ or $Mavs^{-/-}$ mice were prepared as described previously[9,31]. Cells were suspended in RPMI-1640 (Invitrogen) supplemented with 10% heat-inactivated FCS and antibiotics and stimulated with the indicated RNAs. Twenty-four hours after stimulation, culture supernatants were collected and analysed for cytokine levels by ELISA or Cytometric Bead Array (CBA). ELISA kits for mouse IFN-α and IFN-β were purchased from PBL Biomedical Laboratories. CBA flex sets for mouse IL-6 and TNF-α were purchased from BD Bioscience. Experiments were performed according to the manufacturer's instructions and samples were analysed using the Facs Aria (BD Bioscience).

Confocal microscopy. HeLa cells (1.0×10^5 cells per well) were cultured on microcover glasses (Matsunami Glass Ind., Ltd) in a 12-well plate. Three hours after seeding, cells were transfected with GFP-fused Rab5a or Lamp1 using BacMam systems (Cell Light Early Endosomes-GFP BacMam 2.0 or Cell Light Lysosomes-GFP BacMam 2.0, Life technologies) or left untreated. Sixteen hours after transfection, cells were incubated with 15 μg ml^{-1} Cy3-labelled cM362, cM362-dsRNAs or dsRNAs for 30 min at 4 °C. Cells were washed twice and further incubated at 37 °C. And then, cells were fixed with 4% paraformaldehyde at the time points indicated. The coverslips were mounted onto slide glass with Prolong Gold with DAPI for nuclei staining. Cells were visualized at a × 63 magnification using a Zeiss LSM520 META microscope (Carl Zeiss Microscopy GmbH).

Quantitative PCR (qPCR). Total RNA was extracted using the Trizol reagent (Qiagen) and reverse-transcribed using a high-capacity cDNA Reverse Transcripition kit (Applied Biosystems) and random primers according to the manufacturer's instructions. QPCR was performed using specific primers for mouse *GAPDH, IFN-β, IL-6* and *TNF-α* (Supplementary Table 5) and the Step One Real-time PCR system (Applied Biosystems).

Mice. $Ticam1^{-/-}$ and $Mavs^{-/-}$ mice were made in our laboratory and back-crossed more than eight times to adapt C57BL/6 background[9,10]. Inbred C57BL/6 WT mice were purchased from CLEA Japan. $Tlr3^{-/-}$ mice were kindly provided by Dr S. Akira (Osaka University). Mice were maintained under specific pathogen-free conditions in the animal facility of the Hokkaido University Graduate School of Medicine. Female mice 6–12 weeks of age were used in all experiments, all of which were performed according to the guidelines issued by the Hokkaido University Animal Care and Use Committee.

***In vivo* mouse cytokine assay.** Wild-type and $Tlr3^{-/-}$ mice (9 weeks) were injected i.p. with 50 μl (50 μg) poly(I:C), cM362-139 (IVT) or cM362-140, and blood was collected from the tail vein at timed intervals. Cytokine levels in sera were measured using a CBA. In some cases, wild-type and $Ticam1^{-/-}$ mice were s.c. injected with 75 μl (75 μg) poly(I:C) or cM362-140. After 6 h, mice were killed and draining inguinal LN, axillary LN and spleen were harvested[10]. *IFN-β, IL-6* or *TNF-α* mRNA expression in these lymphoid organs was measured by qPCR.

Tumour challenge and sODN-dsRNA treatment. Mice 6–10 weeks of age were used in all experiments. Mice were shaved at the back and injected s.c. with 200 μl of 6×10^5 B16D8 cells in PBS (−). Tumour volumes were measured at regular intervals using a caliper[9]. Tumour volume was calculated using the following formula: tumour volume (cm^3) = (long diameter) × (short diameter)^2 × 0.4. 75 μl (75 μg) sODN-dsRNAs or distilled water with no detectable LPS was mixed with *in vivo*-JetPEI (Polyplus), a polymer-based transfection reagent, according to the manual and then injected s.c. around the tumour. Treatment was started when the average tumour volume of 0.4–0.6 cm^3 was reached. To deplete NK cells, we injected titrated anti-NK1.1 ascites (PK136) i.p. in tumour-bearing mice the day before sODN-dsRNA treatment. Depletion of $NK1.1^+$ cells was verified by flow cytometory.

In the case of EG7 cell challenge, mice were injected s.c. with 200 μl of 2×10^6 syngenic EG7 cells in PBS (−). When the average tumour volumes reached ~0.6 cm^3, 50 μl of 100 μg endotoxin-free ovalbumin in PBS (−) with or without 50 μl of 50 μg poly(I:C) or sODN-dsRNA was injected s.c. around the tumour. PBS (−) (100 μl) was used as a control. Treatments were performed twice per week.

CTL activity in tumour-bearing mice after adjuvant therapy. Female mice 6–10 weeks of age were used for this study. Splenocytes were harvested from tumour-bearing mice at 7 days after the last adjuvant treatment. In the case of tumour-free settings, spleen and inguinal LN cells were harvested from wild-type or $Ticam1^{-/-}$ mice 4 days after the last adjuvant injection. The cells were stained with FITC-CD8α (1:200), PerCP/Cy5.5-7AAD (1:200), APC-CD3ε (1:200) and PE-OVA-tetramer (1:50) to detect Ag-specific $CD8^+$ T cells. To evaluate cytokine production, splenocytes (2×10^6 per 200 μl per well) were cultured for 3 days in the presence of 100 nM OVA peptide (SL8: SIINFEKL) or control WT1 peptide (Db126: RMFPNAPYL) and IFN-γ production was analysed with CBA or ELISA. To assess the cytotoxic activity of CTLs, splenocytes (1×10^6 per ml) were co-cultured with mitomycin C-treated EG7 cells (5×10^5 per ml) in the presence of 10 U ml^{-1} IL-2 for 5 days. Then, the cells were incubated with ^{51}Cr-labelled EG7 or C1498 cells for 4 h and determined cytotoxic activity[10]. The cytotoxicity was calculated by this formula: Cytotoxicity (%) = [(experimental release − spontaneous release)/(total release—spontaneous release)] × 100.

Cytotoxic activity assay of NK cells. Mice bearing B16 tumour were injected s.c. with cM362-139(IVT) mixed with *in vivo*-JetPEI. After 18 h, mice were killed and $DX5^+$ NK cells were isolated from spleen using DX5-positive selection microbeads (Miltenyi) according to the manual[9]. B16 cells were labelled with ^{51}Cr for 1 h and then washed three times with medium. $DX5^+$ cells and ^{51}Cr-labelled B16 cells were co-cultured at the indicated ratio[31]. After 4 h, supernatants were harvested and ^{51}Cr release was measured in each sample. Specific lysis was calculated by the following formula: cytotoxicity (%) = [(experimental release − spontaneous release)/(total release − spontaneous release)] × 100.

Statistical analysis. The significance of differences between groups was determined by the Student's *t*-test. In tumour-implant or -free mouse experiments, one-way analysis of variance with Bonferroni's multiple-comparison test or Dunnett's test was performed to analyse statistical significance.

References

1. Akira, S., Uematsu, S. & Takeuchi, O. Pathogen recognition and innate immunity. *Cell* **124,** 783–801 (2006).
2. Gürtler, C. & Bowie, A. G. Innate immune detection of microbial nucleic acids. *Trends Microbiol.* **21,** 413–420 (2013).
3. Seya, T. *et al.* Role of Toll-like receptors and their adaptors in adjuvant immunotherapy for cancer. *Anticancer Res.* **23,** 4369–4376 (2003).
4. Matsumoto, M. & Seya, T. TLR3: interferon induction by double-stranded RNA including poly(I:C). *Adv. Drug Deliv. Rev.* **60,** 805–812 (2008).
5. Levine, A. S. & Levy, H. B. Phase I-II trials of poly IC stabilized with poly-L-lysine. *Cancer Treat. Rep.* **62,** 1907–1912 (1978).
6. Galluzzi, L. *et al.* Trial watch: experimental Toll-like receptor agonists for cancer therapy. *OncoImmunology* **1,** 699–716 (2012).
7. Lvovsky, E. A., Mossman, K. L., Levy, H. B. & Dritschilo, A. Response of mouse tumor to interferon inducer and radiation. *Int. J. Radiat. Oncol. Biol. Phys.* **11,** 1721–1725 (1985).
8. Talmadge, J. E. *et al.* Immunotherapeutic potential in murine tumor models of polyinosinic-polycytidylic acid and poly-L-lysine solubilized by carboxymethyl cellulose. *Cancer Res.* **45,** 1066–1072 (1985).
9. Akazawa, T. *et al.* Antitumor NK activation induced by the Toll-like receptor 3-TICAM-1 (TRIF) pathway in myeloid dendritic cells. *Proc. Natl Acad. Sci. USA* **104,** 252–257 (2007).
10. Azuma, M., Ebihara, T., Oshiumi, H., Matsumoto, M. & Seya., T. Cross-priming for antitumor CTL induced by soluble Ag + polyI:C depends on the TICAM-1 pathway in mouse CD11c(+)/CD8α(+) dendritic cells. *Oncoimmunology* **1,** 581–592 (2012).
11. Sabbatini, P. *et al.* Phase I trial of overlapping long peptides from a tumor self-antigen and poly-ICLC shows rapid induction of integrated immune response in ovarian cancer patients. *Clin. Cancer Res.* **18,** 6497–6508 (2012).
12. Yoneyama, M., Onomoto, K. & Fujita, T. Cytoplasmic recognition of RNA. *Adv. Drug Deliv. Rev.* **60,** 841–846 (2008).
13. Dixit, E. & Kagan, J. C. Intracellular pathogen detection by RIG-I-like receptors. *Adv. Immunol.* **117,** 99–125 (2013).
14. Matsumoto, M. *et al.* Subcellular localization of Toll-like receptor 3 in human dendritic cells. *J. Immunol.* **171,** 3154–3162 (2003).
15. Sun, J. C., Beilke, J. N. & Lanier, L. L. Adaptive immune features of natural killer cells. *Nature* **457,** 557–561 (2009).
16. Fernandez, N. C. *et al.* Dendritic cells directly trigger NK cell functions: cross-talk relevant in innate anti-tumor immune responses in vivo. *Nature Med.* **5,** 405–411 (1999).
17. Schulz, O. *et al.* Toll-like receptor 3 promotes cross-priming to virus-infected cells. *Nature* **433,** 887–892 (2005).
18. Villadangos, J. A. & Shortman, K. Found in translation: the human equivalent of mouse CD8 + dendritic cells. *J. Exp. Med.* **207,** 1131–1134 (2010).
19. Edelson, B. T. *et al.* Peripheral CD103 + dendritic cells form a unified subset developmentally related to CD8alpha + conventional dendritic cells. *J. Exp. Med.* **207,** 823–836 (2010).
20. Jongbloed, S. L. *et al.* Human CD141 + (BDCA-3) + dendritic cells (DCs) represent a unique myeloid DC subset that cross-presents necrotic cell antigens. *J. Exp. Med.* **207,** 1247–1260 (2010).
21. Kato, H. *et al.* Differential roles of MDA5 and RIG-I helicases in the recognition of RNA viruses. *Nature* **441,** 101–105 (2006).
22. Okahira, S. *et al.* Interferon-beta induction through Toll-like receptor 3 depends on double-stranded RNA structure. *DNA Cell Biol.* **24,** 614–623 (2005).
23. Itoh, K., Watanabe, A., Funami, K., Seya, T. & Matsumoto, M. The clathrin-mediated endocytic pathway participates in dsRNA-induced IFN-beta production. *J. Immunol.* **181,** 5522–5529 (2008).
24. Liu, L. *et al.* Structural basis of Toll-like receptor 3 signaling with double-stranded RNA. *Science* **320,** 379–381 (2008).
25. Shingai, M. *et al.* Differential type I IFN-inducing abilities of wild-type versus vaccine strains of measles virus. *J. Immunol.* **179,** 6123–6133 (2007).
26. Miyake, T. *et al.* Poly I:C-induced activation of NK cells by CD8 alpha + dendritic cells via the IPS-1 and TRIF-dependent pathways. *J. Immunol.* **183,** 2522–2528 (2009).
27. Zhang, Z. *et al.* DDX1, DDX21, and DHX36 helicases form a complex with the adaptor molecule TRIF to sense dsRNA in dendritic cells. *Immunity* **34,** 866–878 (2011).
28. Gauzzi, M. C., Del Cornò, M. & Gessani, S. Dissecting TLR3 signalling in dendritic cells. *Immunobiology* **215,** 713–723 (2010).
29. Conforti, R. *et al.* Opposing effects of Toll-like receptor (TLR3) signaling in tumors can be therapeutically uncoupled to optimize the anticancer efficacy of TLR3 ligands. *Cancer Res.* **70,** 490–500 (2010).
30. Paone, A. *et al.* Toll-like receptor 3 triggers apoptosis of human prostate cancer cells through a PKC-alpha-dependent mechanism. *Carcinogenesis* **29,** 1334–1342 (2008).
31. Ebihara, T. *et al.* Identification of a polyI:C-inducible membrane protein that participates in dendritic cell-mediated natural killer cell activation. *J. Exp. Med.* **207,** 2675–2687 (2010).
32. Alexopoulou, L., Holt, A. C., Medzhitov, R. & Flavell, R. A. Recognition of double stranded RNA and activation of NF-kappaB by Toll-like receptor 3. *Nature* **413,** 732–738 (2001).
33. Matsumoto, M., Kikkawa, S., Kohase, M., Miyake, K. & Seya, T. Establishment of a monoclonal antibody against human Toll-like receptor 3 that blocks double-stranded RNA-mediated signaling. *Biochem. Biophys. Res. Commun.* **293,** 1364–1369 (2002).
34. Shime, H. *et al.* Toll-like receptor 3 signaling converts tumor-supporting myeloid cells to tumoricidal effectors. *Proc. Natl. Acad. Sci. U. S. A.* **109,** 2066–2071 (2012).
35. Oshiumi, H., Matsumoto, M., Funami, K., Akazawa, T. & Seya, T. TICAM-1, an adaptor molecule that participates in Toll-like receptor 3-mediated interferon-beta induction. *Nat. Immunol.* **4,** 161–167 (2003).
36. Yoneyama, M. *et al.* The RNA helicase RIG-I has an essential function in double-stranded RNA-induced innate antiviral responses. *Nat. Immunol.* **5,** 730–737 (2004).
37. Seya, T., Azuma, M. & Matsumoto, M. Targeting TLR3 with no RIG-I/MDA5 activation is effective in immunotherapy for cancer. *Expert Opin. Ther. Targets.* **17,** 533–544 (2013).
38. Hornung, V. *et al.* RNA is the ligand for RIG-I. *Science* **314,** 994–997 (2006).
39. Pichlmair, A. *et al.* RIG-I-mediated antiviral responses to single-stranded RNA bearing 5′-phosphates. *Science* **314,** 997–1001 (2006).
40. Tatematsu, M., Nishikawa, F., Seya, T. & Matsumoto, M. Toll-like receptor 3 recognizes incomplete stem structures in single-stranded viral RNA. *Nat. Commun.* **4,** 1833 (2013).
41. Jelinek, I. *et al.* TLR3-specific double-stranded RNA oligonucleotide adjuvants induce dendritic cell cross-presentation, CTL responses, and antiviral protection. *J. Immunol.* **186,** 2422–2429 (2011).
42. Caskey, M. *et al.* Synthetic double-stranded RNA induces innate immune responses similar to a live viral vaccine in humans. *J. Exp. Med.* **208,** 2357–2366 (2011).
43. Levy, H. B., Low, L. W. & Rabson, A. S. Inhibition of tumor growth by polyinosinic-polycytidylic acid. *Proc. Natl Acad. Sci. USA* **62,** 357–361 (1969).
44. Levine, A. S., Sivulich, M., Wiernik, P. H. & Levy, H. B. Initial clinical trials in cancer patients of polyriboinosinic-polyribocytidylic acid stabilized with poly-L-lysine, in carboxymethylcellulose [poly(ICLC)], a highly effective interferon inducer. *Cancer Res.* **39,** 1645–1650 (1979).
45. Lin, W. W. & Karin, M. A cytokine-mediated link between innate immunity, inflammation, and cancer. *J. Clin. Invest.* **117,** 1175–1183 (2007).
46. Mata-Haro, V. *et al.* The vaccine adjuvant monophosphoryl lipid A as a TRIF-biased agonist of TLR4. *Science* **316,** 1628–1632 (2007).
47. Sugiyama, T. *et al.* Immunoadjuvant effects of polyadenylic:polyuridylic acids through TLR3 and TLR7. *Int. Immunol.* **20,** 1–9 (2008).
48. Perrot, I. *et al.* TLR3 and Rig-like receptor on myeloid dendritic cells and Rig-like receptor on human NK cells are both mandatory for production of IFN-gamma in response to double-stranded RNA. *J. Immunol.* **185,** 2080–2088 (2010).
49. Gowen, B. B. *et al.* TLR3 is essential for the induction of protective immunity against Punta Toro Virus infection by the double-stranded RNA (dsRNA), poly(I:C12U), but not Poly(I:C): differential recognition of synthetic dsRNA molecules. *J. Immunol.* **178,** 5200–5208 (2007).
50. Jasani, B., Navabi, H. & Adams, M. Ampligen: a potential toll-like 3 receptor adjuvant for immunotherapy of cancer. *Vaccine* **27,** 3401–3404 (2009).
51. Hafner, A. M., Corthésy, B. & Merkle, H. P. Particulate formulations for the delivery of poly(I:C) as vaccine adjuvant. *Adv. Drug Deliv. Rev.* **65,** 1386–1399 (2013).
52. Intlekofer, A. M. & Thompson, C. B. At the bench: preclinical rationale for CTLA-4 and PD-1 blockade as cancer immunotherapy. *J. Leukoc. Biol.* **94,** 25–39 (2013).
53. Desmet, C. J. & Ishii, K. J. Nucleic acid sensing at the interface between innate and adaptive immunity in vaccination. *Nat. Rev. Immunol.* **12,** 479–491 (2012).
54. Jing, X. u., Lapham, J. & Crothers, D. M. Determining RNA solution structure by segmental isotopic labeling and NMR: Application to *Caenorhabditis elegans* spliced leader RNA 1. *Proc. Natl Acad. Sci. USA* **93,** 44–48 (1996).
55. Nishikawa, F., Arakawa, H. & Nishikawa, S. Application of microchip electrophoresis in the analysis of RNA aptamer-protein interactions. *Nucleos. Nucleot. Nucl. Acids* **25,** 369–382 (2006).
56. Nishikawa, F., Murakami, K., Matsugami, A., Katahira, M. & Nishikawa, S. Structural studies of an RNA aptamer containing GGA repeats under ionic conditions using microchip electrophoresis, circular dichroism, and 1D-NMR. *Oligonucleotides* **19,** 179–190 (2009).

Acknowledgements

We are grateful to Dr H. Nankai (GeneDesign, Inc., Osaka) for helping chemical synthesis of RNA. Technical and clerical assistance by Dr R. Hatsugai, and Ms H. Sato in our laboratory is gratefully acknowledged. We appreciate Dr K. Toyoshima (RIKEN, Tokyo) for organizing the start of this project.

Author contributions

M.M. and T.S. conceived and designed the experiments. M.T., F.N., M.A., N.I., A.M.-S. and H.S. performed the experiments. M.M. conducted the project. M.M. and T.S. analysed data and wrote the paper.

Additional information

Supplementary Information accompanies this paper at http://www.nature.com/naturecommunications

Competing financial interests: The authors declare no competing financial interests.

Reprints and permission information is available online at http://npg.nature.com/reprintsandpermissions/

How to cite this article: Matsumoto, M. *et al.* Defined TLR3-specific adjuvant that induces NK and CTL activation without significant cytokine production *in vivo*. *Nat. Commun.* 6:6280 doi: 10.1038/ncomms7280 (2015).

VIRAL IMMUNOLOGY
Volume 27, Number 6, 2014

Pp. 285–294
DOI: 10.1089/vim.2013.0140

The J6JFH1 Strain of Hepatitis C Virus Infects Human B-Cells with Low Replication Efficacy

Masato Nakai,[1,2] Tsukasa Seya,[1] Misako Matsumoto,[1] Kunitada Shimotohno,[3] Naoya Sakamoto,[2] and Hussein H. Aly[1,*]

Abstract

Hepatitis C virus (HCV) infection is a serious health problem worldwide that can lead to hepatocellular carcinoma or end-stage liver disease. Current treatment with pegylated interferon, ribavirin, and NS3/4A protease inhibitor would lead to a good prognosis in a large population of patients, but there is still no effective vaccine for HCV. HCV robustly infects hepatocytes in the liver. However, extrahepatic manifestations such as mixed cryoglobulinemia, a systemic immune complex-mediated disorder characterized by B-cell proliferation, which may evolve into overt B-cell non-Hodgkin's lymphoma, have been demonstrated. HCV-RNA is often found to be associated with peripheral blood lymphocytes, suggesting a possible interaction with peripheral blood mononuclear cells (PBMCs), especially B-cells with HCV. B-cell HCV infection was a matter of debate for a long time, and the new advance in HCV *in vitro* infectious systems suggest that exosome can transmit HCV genome to support "infection." We aimed to clarify the susceptibility of primary B-cells to HCV infection, and to study its functional effect. In this article, we found that the recombinant HCV J6JFH1 strain could infect human B-cells isolated from the peripheral blood of normal volunteers by the detection of both HCV-negative-strand RNA by reverse transcription polymerase chain reaction, and NS5A protein. We also show the blocking of HCV replication by type I interferon after B-cell HCV infection. Although HCV replication in B-lymphocytes showed lower efficiency, in comparison with hepatocyte line (Huh7) cells, our results clearly demonstrate that human B-lymphocytes without other non-B-cells can actually be infected with HCV, and that this interaction leads to the induction of B-cells' innate immune response, and change the response of these cells to apoptosis.

Introduction

CHRONIC INFECTION BY HEPATITIS C VIRUS (HCV) is the major cause of liver cirrhosis and hepatocellular carcinoma. About 3.1% of the global population is infected with HCV (50). Historically, a combination therapy with pegylated interferon (IFN) and ribavirin was used for patients infected with genotype 1 HCV. NS3/4A protease inhibitors were recently developed in addition to pegylated IFN and ribavirin, and their combinations have been clinically tried for HCV treatment since then. Although >70% of patients with high viral loads of HCV genotype 1b have a sustained viral response by the therapy using simeprevir or telaplevir with pegylated IFN and ribavirin (17,22), the remaining patients fail to eliminate the virus, and drug resistance remains an issue that must be resolved. Recent development of direct-acting antiviral (DAA) drugs (such as daclatasvir, asunaprevir, and sofosbuvir) are a promising therapeutic option beyond IFN in the treatment of HCV patients (6,32).

HCV is a single-stranded, positive-sense RNA virus in the Hepacivirus genus of the Flaviviridae family. Although HCV is known to infect hepatocytes in the liver and induce hepatitis *in vivo*, *in vitro* cultured primary hepatocytes barely support the HCV life cycle: only hepatoma Huh7 cells and its subclones can efficiently maintain the HCV life cycle of a very limited number of HCV strains *in vitro* (53).

Chronic hepatitis patients with HCV sometimes show other extrahepatic complications such as lymphoproliferative diseases (LPD), including cryoglobulinemia and B-cell malignant lymphoma, autoimmune diseases, and dermatitis (1,12,15,16). Epidemiological analysis shows that chronic HCV patients have higher rates of LPDs than non-HCV-infected populations (36,48,52). Several reports suggested that some lymphotropic HCV strains effectively infected human

Departments of [1]Microbiology and Immunology, and [2]Gastroenterology, Hokkaido University Graduate School of Medicine, Kita-ku, Japan.
[3]Research Center for Hepatitis and Immunology, National Center for Global Health and Medicine, Ichikawa, Japan.
*Present affiliation: Department of Virology II, National Institute of Infectious Diseases, Toyama, Tokyo, Japan.

lymphocytes (20,47), leading to the above-mentioned abnormalities. Infection of lymphocytes with HCV has been a matter of debate for a long time. More than one decade ago, several reports described the existence of HCV-RNA in peripheral blood mononucleated cells (PBMCs) (30,40). The detection rate of HCV-RNA in PBMCs was increased if patients were infected with human immunodeficiency virus (HIV) together with HCV (44). This phenomenon indicated that immune-suppressive circumstances and/or HIV antigen might enhance the replication activity of HCV in lymphoid cells (44). Moreover, it was reported that continuous release of HCV by PBMCs was detected in HCV-infected patients, especially in HIV co-infected patients (7). In addition to HCV-HIV co-infected patients, a low level of HCV replication could be detected in peripheral lymphoid cells from HCV mono-infected patients after antiviral treatment (34,45). Moreover, it was reported that HCV persisting at low levels long after therapy-induced resolution of chronic hepatitis C remained infectious (34). This continuous viral presence could present a risk of infection reactivation.

It has been reported that HCV replication was detected in various kinds of lymphoid cells. Many reports describing the existence of HCV in B-lymphocytes and B-cell lymphoma have been published (21,25,51). Among B-lymphocytes, CD27+ memory B-lymphocytes were more resistant to apoptosis than CD27− B-lymphocytes. CD27+ B-lymphocytes were reported as a candidate subset of the HCV reservoir in chronic hepatitis C (CH-C) (38). On the other hand, others claimed that distinguishing RNA association from true HCV replication was problematic, together with multiple artifacts complicated detection and quantitation of the replicative intermediate minus strand RNA (29,31), and also the failure of retroviral (37) and lentiviral (8) pseudoparticles bearing HCV envelope glycoproteins (HCVpp) to infect primary B-cells or B-cell lines. This led to continuous debate about HCV infection into B-lymphocytes, and the riddle remained unsolved.

Using the recent progress in HCV infection systems, we intended to clarify this debate and analyze HCV infection in human lymphocytes and its functional results. Here, albeit in a lower efficiency compared to HCV infection into Huh7 cells, we report that two different strains of recombinant HCV viruses could infect primary human lymphocytes not only by the detection of HCV-RNA positive and negative strands proliferation, but also NS5A protein detection, and the detection of the activity of luciferase reporter encoded by the recombinant HCV-genome. Blocking of HCV entry using anti-CD81 antibody (Ab), and replication by IFN-α or NS3/4A protease inhibitors successfully suppressed HCV infection. We also found that HCV infection into B-lymphocytes led to the initiation of host response including apoptosis resistance.

Materials and Methods

Cells and reagents

Huh7.5.1 cells were kindly provided by Dr. Francis V Chisari (The Scripps Research Institute, La Jolla, CA). Cells were cultured in high-glucose Dulbecco's modified Eagle's medium (DMEM ; Gibco/Invitrogen, Tokyo, Japan) supplemented with 2 mM L-Glutamine, 100 U of penicillin/mL, 100 μg of streptomycin/mL, 1× MEM non-essential amino acid (Gibco/Invitrogen), and 10% fetal bovine serum (FBS).

Human peripheral blood mononuclear cells (PBMCs) were obtained from healthy volunteers by density gradient centrifugation using Ficoll Paque plus (GE-Healthcare, Waukesha, WI). CD19+ blood cells (representative of human primary B-cells) and CD19− cells (non-B-cells) were separated by MACS CD19 Beads (Milteny Biotec, Bergisch Gladbach, Germany). Purity of CD19+ B-cells was >95% after two-cycle separation. The cells were cultured in RPMI1640 (Gibco/Invitrogen) supplemented with 100 U of penicillin/mL, 100 μg of streptomycin/mL, and 10% FBS.

The following reagents were obtained as indicated: anti-CD81 Ab (BD Pharmingen, Franklin Lakes, NJ); PE anti-CD80 Ab, APC anti-CD86 Ab, and PE-labeled anti-CD19 Ab (eBioscience, San Diego, CA); recombinant IFN-α (Peprotech, Oak Park, CA); BILN2601 (Behringer, Willich, Germany); and Viaprobe 7AAD (BD Bioscience) and Annexin-V-Fluos (Roche, Mannheim, Germany).

Virus propagation

pJ6-N2X-JFH1 was kindly provided from Dr. Takaji Wakita (National Institute of Infectious Diseases, Tokyo) (2). pJc1-GLuc2A was gifted from Dr. Brett D. Lindenbach (Yale University, New Haven) (41). *In vitro* RNA transcription, gene transfection into Huh7.5.1 cells, and preparation of J6JFH1 and Jc1/GLuc2A viruses were performed as previously reported (53). Briefly, the HCV cDNA in plasmids were digested by XBaI and transcribed by T7 Megascript Kit (Invitrogen, Carlsbad, CA). RNA transfection into Huh7.5.1 was performed by electroporation using Gene Pulser II (Bio-Rad, Berkeley, CA) at 260 V and 950 Cap. Culture supernatant were collected on days 3, 5, 7, and 9 of postelectroporation, and concentrated with an Amicon Ultra-15 Centrifugal Filter unit (Millipore, Billerica, MA). The titer of HCVcc was checked by the immunofluoresence method using NS5A antibody when Huh7.5.1 was reinfected with these HCVcc.

Virus infection

Primary B-cells and non-B-cells were cultured with the J6JFH1 HCV strain at a multiplicity of infection (MOI) = 1–3 for 3 h, and cells were harvested after four extensive washes in culture medium. On days 1–6, cells were collected, washed with 0.25% trypsin-EDTA/saline, and incubated with 0.25% trypsin-EDTA for 5 min at 37°C. Then, suspended cells were collected as a source of total RNA. In some experiments, B-cells were infected with the Jc1/GLuc2A strain at MOI = 5 for 3 h. Cells were washed five times in 1× phosphate buffered saline (PBS), and cultured until day 6 for determination of viral replication as GLuc activity with BioLux Gaussia luciferase assay kits (41).

RNA purification, RT-PCR, and quantitative PCR

Total RNA was extracted by using Trizol Reagent (Invitrogen) according to the manufacturer's instructions. Using 100–400 ng of total RNA as a template, we performed RT-PCR and real-time RT-PCR as previously described (3,4). Primer sets are shown in Supplementary Table S1 and Table S2 (Supplementary Data are available online at www.liebertpub.com/vim).

Real-time PCR was used for quantification of positive-strand and negative-strand HCV RNA. Total Trizol-extracted

RNA was analyzed by RT-PCR with a modification of the previously described strand-specific rTth RT-PCR method (10,13). RT primers for complementary DNA synthesis of positive and negative strand HCV RNA are shown in Supplementary Table S1. Positive-strand and negative-strand HCV PCR amplifications were performed using Power SYBR Green PCR Master Mix (Applied Biosystems, Warrington, UK) with 200 nM of paired primers (Supplementary Table S1). The PCR conditions were 95°C for 10 min, followed by 40 cycles at 95°C for 15 sec and 60°C for 1 min.

Virus production and releasing assay

Primary human B-cells were infected with J6JFH1 at MOI = 1. Six days postinfection, the supernatant was collected ("releasing samples"), cells were repeatedly frozen and thawed, and the supernatant was collected ("assembly samples"). Viral titers of "releasing samples" and "assembly samples" were determined with Huh7.5.1 cells using J6JFH1 virus (MOI = 0.001 and 0.01) as control. Total RNA was recovered from the cells on days 2, 4, and 6, and determined with HCV-RNA to check reinfectivity.

Indirect immunofluorescence

Indirect immunofluorescence (IF) expression of HCV proteins was detected in the infected cells using rabbit IgG anti-NS5A antibody (Cl-1) (3). Goat anti-rabbit Alexa 594 (Invitrogen) was used as secondary Ab. Fluorescence detection was performed on the Zeiss LSM 510 Meta confocal microscope (Zeiss, Jena, Germany) (13).

Luciferase assay

Primary B-cells were infected with Jc1/Gluc2A by using concentrated Medium or Mock Medium (PBS-electropolated Huh7.5.1 medium). Media were collected on days 0, 2, 4, and 6 postinfection, cleared by centrifugation (16,000 *g* for 5 min), and mixed with 0.25 volume of *Renilla* 5 lysis buffer (Promega, Madison, WI) to kill HCV infectivity. GLuc activity was measured on a Berthold Centro LB 960 luminescent plate reader (Berthold Technologies, Bad Wildbad, Germany) with each 20 μL sample injected with 50 μL BilLux Gaussia Luciferase Assay reagent (New England Biolabs, Ipswich, MA), integrated over 1 sec.

Cell survival assay

Apoptosis assay: Primary B cells were infected with J6JFH1 virus. Cells were collected 48 h after infection, stained by 7AAD Cell Viability assay kit and Annexin V, and analyzed by FACS Calibur (BD) (13).

ATP assay

Primary B-cells were infected with J6JFH1 virus or Mock concentrated medium. Cells were resuspended and cultured at Lumine plate (Berthold Technologies) postinfection. ATP activities were determined 72 h later using CellTiter-Glo® Luminescent Cell Viability Assay (Promega) according to the manufacturer's protocol.

miRNA detection

Total RNA was extracted by using Qiazol Reagent (Invitrogen). These RNA was purificated and reverse transcripted to cDNA by using the miScript II RT Kit. Synthesized cDNA was used to determine the expression levels of miR-122 (24). Total miRNA was prepared by using Qiazol and miScript II RT kit (Invitrogen), and miR-122 expression was determined by using miScript SYBR Green PCR Kit and miScript Primer Assay (Invitrogen) according to the manufacturer's protocol. U6 small nuclear RNA was used as an internal control.

Results

J6JFH1 infects and replicates in primary B-cells

To address HCV infectivity into primary B-cells, PBMC were isolated from the blood of healthy volunteers and were sorted into CD19+ cells (primary B-lymphocytes) and CD19− cells (non-B-cells). Their purities were >95%. These cells were then incubated with the J6JFH1 HCV. Total RNA was collected on days 2, 4, and 6. The Huh7.5.1 strain was used as positive control. Both Huh7.5.1 and primary B-cells, but not non-B-cells, showed an increase in intracellular HCV-RNA titer, albeit primary B-cells showed lower efficiency than Huh7.5.1 (Fig. 1A). We adjusted the HCV-RNA values using GAPDH as an internal control (Fig. 1B). To confirm J6JFH1 replication in primary B-cells using IF, we also measured the expression of HCV-NS5A, which is a nonstructural protein produced only by the virus secondary to replication. Although the expression was far lower than Huh7.5.1 cells, we managed to detect the NS5A expression in J6JFH1 infected primary B-cells (Fig. 1C).

We examined what kinds of HCV-entry receptors human primary B-cells expressed in our setting. Human CD81, SRB1, and NPC1L1 were expressed, but not the tight junction proteins claudin1 and occludin in mRNA levels (Supplementary Fig. S1). We could not detect miR122 in primary B-cells (Supplementary Fig. S2), expression of which makes the cells permissive to HCV (24). Human CD81 is a primary entry receptor for HCV in hepatocytes (42). Blocking human CD81 by its specific Ab resulted in blockage of HCV infection into primary B-cells, as shown by the suppression of HCV-RNA titer (Fig. 2), suggesting that HCVcc particles enter B-cells also using CD81 receptor. HCV-RNA titer was not suppressed by non-specific Ab (data not shown).

We then examined the effect of the different drugs used to suppress HCV replication (recombinant human IFN, and HCV protease inhibitor, BILN2601). Inhibition of HCV-RNA replication was observed when B-cells were treated with rhIFN-α or BILN2601 (Fig. 2) after infection. BILN2601 showed efficient inhibitory effect on replication of HCV RNA in Huh7.5.1 cells (Supplementary Fig. S3). As control studies, we confirmed that the production of HCV RNA was reduced in Huh7.5.1 cells by CD81 Ab, IFN-α, or BLIN2601 (Supplementary Fig. S4). In both Huh 7.5.1 and B-cells, BLIN2601 most effectively block HCV replication. These data reinforce that HCV is actually replicating in primary B-cells, and that activation of innate immunity by IFN treatment or blocking the NS3/4A protease function is a critical factor in blocking HCV replication in primary B-cells. These data suggest that our system can be used for screening the function of different inhibitors on HCV replication in B-cells.

HCV negative-strand RNA detected in human B-cells

To confirm HCV replication in primary B-cells further, we tested for an increase of negative-strand HCV-RNA after

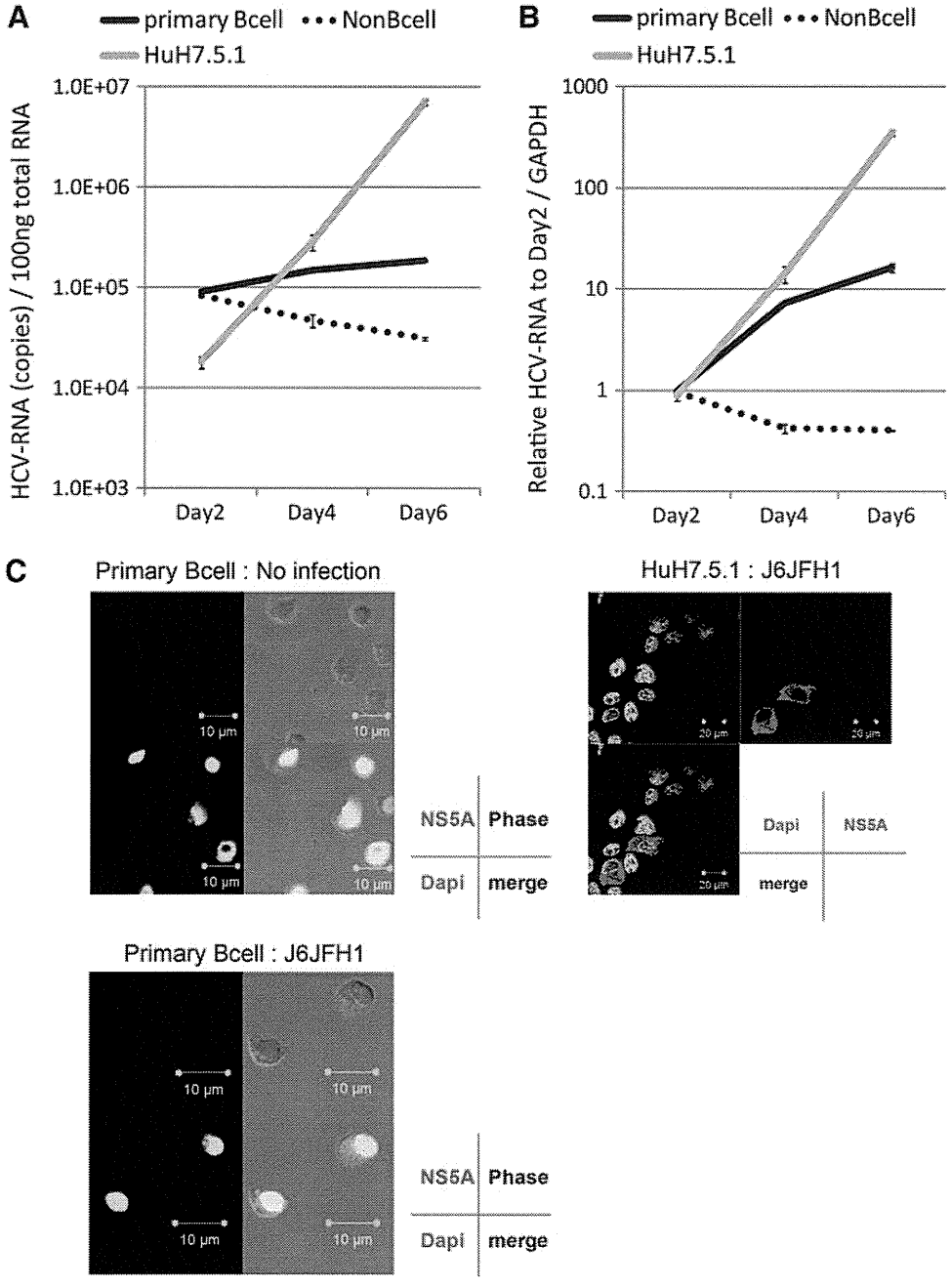

FIG. 1. J6JFH1 infects human peripheral blood B-cells. Human B-cells (CD19+ cells) and non-B-cells (CD19− cells) were separated by MACS as described in Materials and Methods. Primary B-cells, non-B-cells, and Huh7.5.1 cells were infected with J6JFH1 at MOI = 1 for 3 h. After infection, cells were washed twice with culture medium and continued culture. On days 2, 4, and 6, total RNA was collected and HCV-derived RNA was determined by reverse transcription polymerase chain reaction (RT-PCR). GAPDH was used as internal control. **(A)** HCV-RNA not adjusted by GAPDH. **(B)** HCV-RNA adjusted by GAPDH. **(C)** Immunofluorescence analysis of J6JFH1-infected human B-cells and Huh7.5.1 cells. Six days postinfection. Red, NS5A; blue: Dapi; phase: phase-shift microscope.

infection, since the negative-strand RNA is not yielded if HCV particles or RNA just adhere to the cell surface of human primary B-cells without internalization (9,14,19,35, 42,43). We measured the synthesis of plus-strand and minus-strand HCV-RNA separately using strand-specific RT primers and rTth polymerase as previously described (4). The titer increase of minus-strand HCV-RNA indicates HCV-RNA replication. As shown in Figure 3, both minus- and plus-strand HCV-RNA increased time dependently in primary B-cells, and both types of RNA concomitantly decreased in non-B-cells (Fig. 3A and B). Plus- and minus-strand RNA were exponentially increased in Huh7.5.1 cells infected with J6JFH1 (Fig. 3C). These results indicated that primary human B-cells supported J6JFH1 infection and replication, although viral replication levels in B-cells were modest compared with those in Huh7.5.1 cells. These results

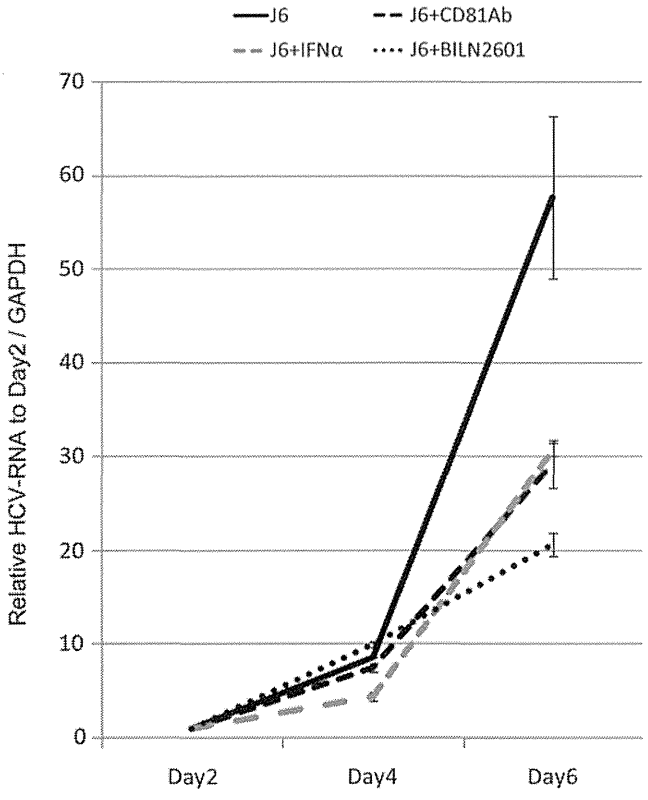

FIG. 2. J6JFH1 B-cell infection is blocked by anti-CD81 Ab, IFN-α, or an NS3/4A inhibitor. Anti-CD81 neutralizing Ab (20 μg/mL) was added to the B-cell culture 1 h before infection. Otherwise, recombinant IFN-α rhIFN-α, 200 IU/mL) or BLIN2601 (250 nM, which is IC75; see Supplementary Fig. S3) was added 1 h after infection. On days 2, 4, and 6, total RNA was extracted, and HCV-RNA was determined by RT-PCR. The values were adjusted by GAPDH.

may reflect the fact that the NS5A protein is difficult to detect in infected B-cells using IF assay.

B-cells can be infected with different HCV strains

We next used the Jc1/GLuc2A strain to investigate whether different HCV strains infect primary B-cells. Primary B-cells, non-B-cells (data not shown), and Huh7.5.1 cells were infected with the Jc1/GLuc2A strain. After five washes, supernatant was collected (day 0 samples). On days 2, 4, and 6, medium was collected. Luciferase activity was determined for all samples by luminescence (GLuc). GLuc activity and detection of RNA increased exponentially in Huh7.5.1 cells infected with the Jc1/GLuc2A strain (Fig. 4A). GLuc activity on day 4 to day 6 increased more in primary B-cells than in non-B-cells (Fig. 4B). These results suggest that HCV replication is substantial, but low in the HCV line Jc1/GLuc2A.

B-cells neither produce nor release detectable level of HCV infectious particles

We collected supernatants of J6JFH1-infected primary human B-cells to measure productive infection in B-cells. The supernatant was then added to culture of Huh7.5.1 cells, and we compared infection with control Huh7.5.1 cells, whose cells were infected with a low MOI (0.01 and 0.001) of J6JFH1 collected from media of the infected Huh7.5.1 cells. HCV-RNA titer in the Huh7.5.1 titrating cells was decreased over time after co-culture with B-cell supernatants obtained from either "releasing samples" "assembly samples." In contrast, HCV-RNA titers were slightly increased over time in the Huh7.5.1 titrating cells that had been infected with medium collected from low MOI-J6JFH1-infected Huh7.5.1 cells (Fig. 5). These results indicated that primary human B-cells were infected with J6JFH1 but failed to assemble or produce particles into the supernatant.

Host response to HCV infection into primary B-cells

Next, we determined whether B-cell activation was induced in HCV-infected B-cells that survived under HCV infection. We measured induction of CD80 and CD86 as B-cell activation markers. After 2–3 days of infection, the CD80/86 levels on B-cells treated with J6JFH1 were compared with those treated with medium from mock-infected cells (concentrated Huh7.5.1 medium) by FACS analysis (Fig. 6A). We found that CD80/86 were upregulated in infected cells compared to mock-infected cells.

Since B-cell lymphoma is a known complication of chronic HCV infection (20,36) and acquiring apoptotic resistance is essential for the development of cancer (21,51,38), we measured the ability of B-cells to escape apoptosis after HCV infection. B-cell apoptosis spontaneously occurs during culture at 37°C. The percent of apoptosis of primary B-cells was decreased in FACS analysis using 7AAD viaprobe + annexinV (Fig. 6B) and ATP assays postinfection (Fig. 6C). These results suggest that primary B-cells are protected from apoptosis by infection with HCVcc. It has been reported that B-cells were vulnerable to apoptotic cell death at various stages of peripheral differentiation and during signal responses (18). Thus, the results infer that HCV stimulation interferes with B-cell apoptotic signal in human B-cells.

Discussion

We show evidence suggesting that human peripheral B-cells can be infected with HCV strains. Establishment of J6JFH1 infection was evaluated by minus-strand PCR amplification, production of core and NS5A proteins, and protection from apoptosis. An increase in HCV RNA in B-cells was inhibited by an exogenously added antibody against CD81 that blocked HCV receptor function. Furthermore, blocking HCV replication in B-cells by type I IFN and NS3/4A protease inhibitor confirmed the presence of HCV infection/replication in human B-cells. The results were corroborated with another HCV strain, Jc1/GLuc2A. Although we failed to establish an EBV-transformed B-cell line to reproduce HCV infection of B-cells, peripheral blood B-cells were infected with J6JFH1 in 12 independent experiments.

One of the well-known complications of chronic HCV infection is LPD, including cryoglobulinemia and B-cell malignant lymphoma, indicating the involvement of B-cells in the course of the disease (1,12,15,16). However, many reports describing the existence of the HCV genome in B-cells and lymphomas (21,25,51) and HCV replication in B-cells have been controversial due to multiple artifacts complicated in detection and quantitation of the replicative

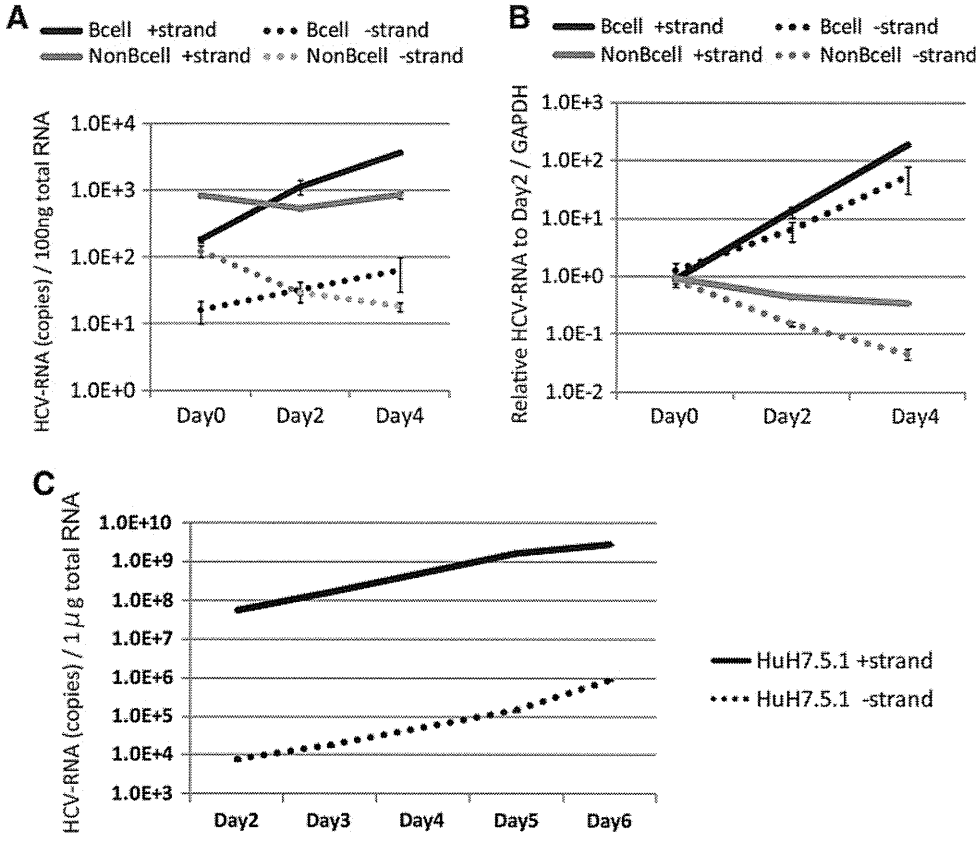

FIG. 3. HCV negative strand RNA is detected in human B-cells. By using rTth methods, HCV strand-specific RNA was determined in J6JFH1-infected human B-cells. **(A)** Not only plus strand HCV-RNA but also minus strand HCV-RNA were increased in a time-dependent manner in human B-cells. **(B)** When HCV-RNA was adjusted by GAPDH that was used as an internal control, HCV-RNAs in B-cells were substantially increased compared with those in non-B-cells. **(C)** Plus and minus strand HCV-RNAs were efficiently amplified in J6JFH1-infected Huh 7.5.1 cells. The level of HCV-RNA exponentially increased in this hepatocyte line.

intermediate minus strand RNA (29,31). This has led to a continuous debate about HCV infection in B-lymphocytes.

HCV entry into B-cells has also been previously reported to be absent because retroviral (37) and lentiviral (8) pseudoparticles bearing HCV envelope glycoproteins (HCVpp) did not infect primary B-cells or B-cell lines. In our study, while we succeeded in infecting Huh7.5.1 cells efficiently with retroviral pseudoparticles for expressing both HCV E1/E2 and the control VSV-G, we failed to establish the same infection in B-cells, suggesting that the block of pseudoparticle entry into B-cells is not related to HCV glycoproteins alone.

Total PBMCs reportedly facilitate HCV attachment but not internalization (42), so HCV infection of B-cells is abrogated in total PBMCs (35). The cause of HCV absorption is unclear, but incomplete sets of HCV receptors in non-B PBMC cells permit attachment of HCV without internalization. B-cells possess CD81, SRBI, LDL-R, and NPC1L1. Because B-cells are not adherent cells, they do not express claudin 1 and occludin, which forms a receptor complex for HCV (9,14,19,43). Claudin 1 and occludin are components of tight junctions and serve as HCV receptors in human hepatocytes. In infection studies using cells expressing these proteins, however, claudin 1 and occludin only upgrade infection efficacy and are dispensable to infection (5), although CD81 is essential for establishment of infection (42). Lack of claudin 1 and occludin or miR122 might be a cause of the low HCV infection efficiency observed in human B-cells. Function blocking of CD81 by its specific antibody suppressed HCV infection in primary B-lymphocytes, which imply that HCV entry into primary B-lymphocyte is dependent on the direct interaction phenomenon between HCV virus particles and CD81 receptor and is not mediated by other nonspecific (CD81 independent) pathways such as exosomal transfer of HCV from Huh7 cells to nonhepatic cells, such as dendritic cells (46).

Previous report using *in vitro* prepared recombinant HCV JFH1 particles (HCVcc) failed to establish HCV infection in B-lymphocyte cell lines (39). While HCV is known to infect human hepatocytes *in vivo* leading to chronic viral hepatitis, in the *in vitro* conditions, only the combination between Huh7 cells and its derived clones supported robust replication and infection with only JFH1 or its derived chimeras (5). Neither hepatocyte cell lines including primary hepatocytes nor other HCV strains could reproduce HCV infection efficiently *in vitro* (5). These data suggest that the clonal selection of HCV quasispecies by hepatoma Huh7 cells is essential for this robust infection *in vitro*. The situation would be similar to the JFH1 story in B-cell HCV infection.

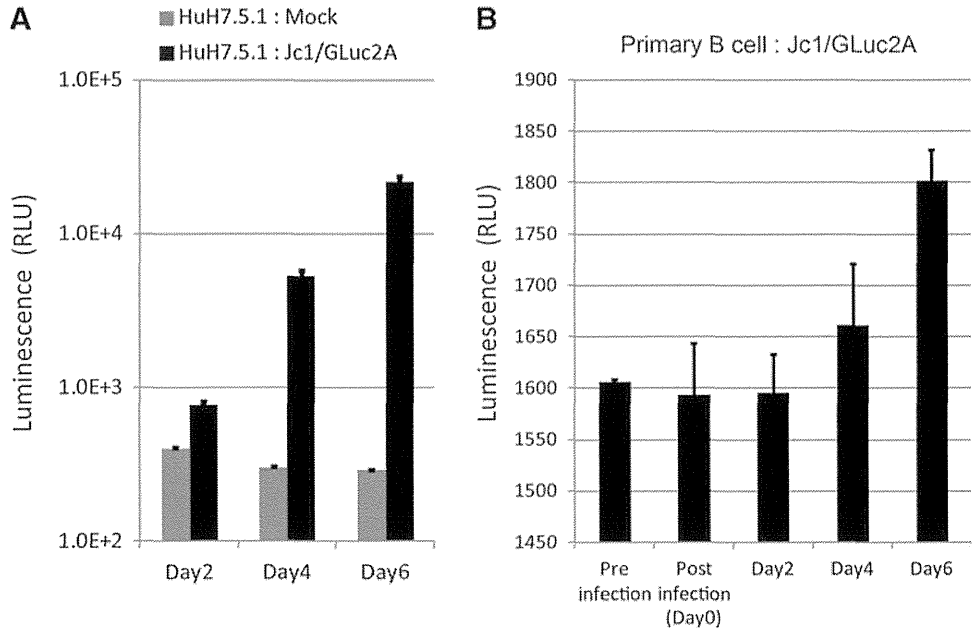

FIG. 4. Jc1/GLuc2A strain infects human B-cells with an increase of Gluc activity. Human B-cells and Huh7.5.1 cells were infected with the JC1/GLuc2A strain that contains secretory luciferase derived from *Gaussia* (GLuc) at MOI = 5. Huh7.5.1 cells were used as control. GLuc activity was increased as time cultured. The GLuc activity was saturated in Huh7.5.1 (**A**). On the other hand, GLuc activity was increased from day 4 in human B-cells (**B**).

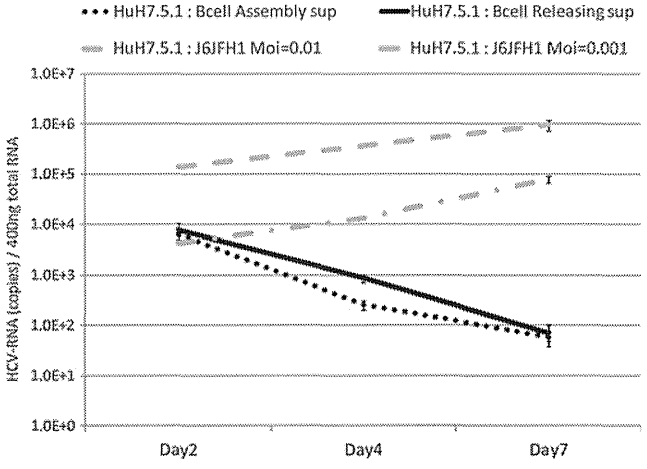

FIG. 5. B-cells infected with J6JFH1 fail to produce virus particles. Human B-cells were infected with J6JFH1 for 3 h, washed twice with phosphate buffered saline (PBS), and cultured. Six days after infection, the supernatant was collected ("releasing samples"). Cells were periodically frozen and thawed five times, and the supernatant was collected ("assembly samples"). For evaluation of the infectious virions, Huh7.5.1 cells were treated with these "releasing samples" or "assembly samples." Similarly, Huh7.5.1 cells were treated with J6JFH1 at low MOI (MOI = 0.01 and 0.001) in parallel. After the treatment, cells were washed and cultured. On days 2, 4, and 7, cells were harvested to collect HCV-RNA. Total RNA was extracted from each samples, and HCV-RNA was determined by RT-PCR methods.

B-cell apoptosis spontaneously occurs during culture at 37°C. We found that B-cell apoptosis was blocked by J6JFH1 infection, as reported previously using Raji cells (11). B-cell apoptosis usually occurs secondary to viral infection, but HCV is particular since apoptotic signaling interferes with infection, leading to protection from cell death. However, B-cell survival was not due to primary infection, because the percent of cells circumventing apoptosis was usually higher than cells infected with HCV. We could not define the pathways that participated in apoptosis regulation by HCV, although a previous report (11) suggested that E2-CD81 engagement was related to B-lymphocyte disorders and weak neutralizing antibody response in HCV patients. Since B-cell lymphoma is a known complication of chronic HCV infection (27), the inability of infected cells to undergo apoptosis can be associated with the development of cancer (28,33,49). In this context, B-cell lymphoma often occurs in mice with Cre-initiated HCV transgenes (26). It is notable that anti-apoptotic effect of HCV core gene was reported in genotype 3a in Huh7 cells (23) and, here, genotype 2a in B-cells. In another report (51), HCV strains established from B-cell lymphoma persistently infected with HCV were genotype 2b. B-cell HCV infection might not be linked to some specific genotypes of HCV.

We believe that our report shows that human primary B-cells can be infected *in vitro* with HCV, and that this infection is dependent on HCV particles binding with its receptor CD81 and is not nonspecific entry (e.g., exosomal mediated). We also show that this infection could be blocked with antibodies interfering with this binding, or with drugs that suppress HCV replication. Although no virion was generated from B-cells in HCV infection, it is still likely that B-cells serve as a temporal reservoir of HCV in the blood circulation. If B-cells permit HCV infection, RNA sensors

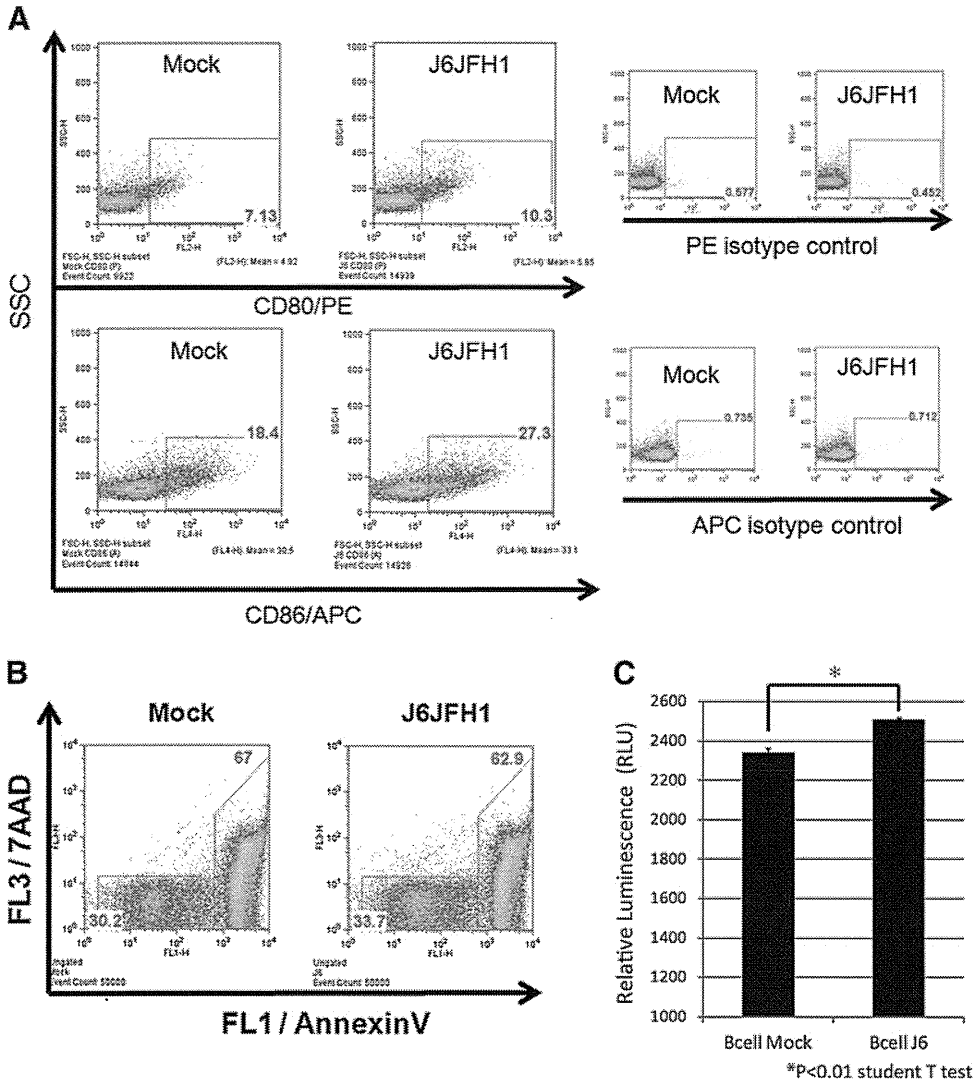

FIG. 6. J6JFH1 infection activates B-cells and protects the cells from apoptosis. Human B-cells were infected with J6JFH1 at MOI = 1 for 3 h, washed twice with PBS, and cultured. Two days after inoculation, cells were washed and suspended with FACS buffer. **(A)** The cells were incubated with PE-conjugated anti-human CD80 antibody, APC-conjugated CD86 antibody, or PE/APC-conjugated mouse IgG1 isotype control for 30 min. Then, the cells were washed and resuspended in FACS buffer. Cells were analyzed by FACS. **(B)** Annexin V and 7AAD viaprobe were added and cultured at 18°C for 10 min. Then, cells were analyzed by FACS. **(C)** 2×10^5 human B-cells were infected with J6JFH1- or Mock-concentrated medium for 3 h. Cells were then washed, resuspended, and cultured in a 96-well white microwell plate. Two days later, ATP activity was determined with a CellTiter-Glo® Luminescent Cell Viability Assay Kit (Promega). ATP activity was adjusted by day 0 ATP activity.

RIG-I and MDA5 in B-cells might recognize HCV RNA and evoke intracellular signaling, including by transcription factors NF-κB and IRF-3/7 (5). Activation of the cytokine network is triggered in human B-cells in response to HCV RNA. In fact, host factors liberated by HCV-infecting B-cells have been previously reported in HCV patients (1,12,15,16,52). Although patients' outcomes would be more than we can be predicted from our results, this system would actually benefit the future study on B-cell–virus interaction.

Acknowledgments

We are grateful to Drs. Frank Chisari (Scripps Research Institute, San Diego, CA) for the Huh7.5.1 cells, Takaji Wakita (National Institute of Infectious Diseases, Tokyo) for supplying the J6JFH1 plasmid, and Brett Lindenbach (Yale University, New Haven, CT) for providing us with the pJc1-GLuc2A HCV strain.

This work was supported in part by Grants-in-Aid from the Ministry of Education, Science, and Culture (Specified Project for "Carcinogenic Spiral") and the Ministry of Health, Labor, and Welfare of Japan, and by the Program of Founding Research Centers for Emerging and Reemerging Infectious Diseases, MEXT. Financial support by the Takeda Science Foundation, the Yasuda Cancer Research Foundation, and the Iskra Foundation are gratefully acknowledged.

Author Disclosure Statement

No competing financial interests exist.

References

1. Agnello V, Chung RT, and Kaplan LM. A role for hepatitis C virus infection in type II cryoglobulinemia. N Engl J Med 1992;327:1490–1495.
2. Aizaki H, Morikawa K, Fukasawa M, *et al.* Critical role of virion-associated cholesterol and sphingolipid in hepatitis C virus infection. J Virol 2008;82:5715–5724.
3. Aly HH, Oshiumi H, Shime H, *et al.* Development of mouse hepatocyte lines permissive for hepatitis C virus (HCV). PLoS One 2011;6:e21284.
4. Aly HH, Qi Y, Atsuzawa K, *et al.* Strain-dependent viral dynamics and virus–cell interactions in a novel *in vitro* system supporting the life cycle of blood-borne hepatitis C virus. Hepatology 2009;50:689–696.
5. Aly HH, Shimotohno K, Hijikata M, and Seya T. *In vitro* models for analysis of the hepatitis C virus life cycle. Microbiol Immunol 2012;56:1–9.
6. Asselah T, and Marcellin P. Second-wave IFN-based triple therapy for HCV genotype 1 infection: simeprevir, faldaprevir and sofosbuvir. Liver Int 2014;34:60–68.
7. Bare P, Massud I, Parodi C, *et al.* Continuous release of hepatitis C virus (HCV) by peripheral blood mononuclear cells and B-lymphoblastoid cell-line cultures derived from HCV-infected patients. J Gen Virol 2005;86:1717–1727.
8. Bartosch B, Dubuisson J, and Cosset FL. Infectious hepatitis C virus pseudo-particles containing functional E1-E2 envelope protein complexes. J Exp Med 2003;197; 633–642.
9. Bartosch B, Vitelli A, Granier C, *et al.* Cell entry of hepatitis C virus requires a set of co-receptors that include the CD81 tetraspanin and the SR-B1 scavenger receptor. J Biol Chem 2003;278:41624–41630.
10. Castet V, Fournier C, Soulier A, *et al.* Alpha interferon inhibits hepatitis C virus replication in primary human hepatocytes infected *in vitro*. J Virol 2002;76:8189–8199.
11. Chen Z, Zhu Y, Ren Y, *et al.* Hepatitis C virus protects human B lymphocytes from Fas-mediated apoptosis via E2-CD81 engagement. PLoS One 2011;6:e18933.
12. Donada C, Crucitti A, Donadon V, *et al.* Systemic manifestations and liver disease in patients with chronic hepatitis C and type II or III mixed cryoglobulinaemia. J Viral Hepat 1998;5:179–185.
13. Ebihara T, Shingai M, Matsumoto M, Wakita T, and Seya T. Hepatitis C virus-infected hepatocytes extrinsically modulate dendritic cell maturation to activate T cells and natural killer cells. Hepatology 2008;48:48–58.
14. Evans MJ, von Hahn T, Tscherne DM, *et al.* Claudin-1 is a hepatitis C virus co-receptor required for a late step in entry. Nature 2007;446:801–805.
15. Ferri C, Caracciolo F, Zignego AL, *et al.* Hepatitis C virus infection in patients with non-Hodgkin's lymphoma. Br J Haematol 1994;88:392–394.
16. Frangeul L, Musset L, Cresta P, Cacoub P, Huraux JM, and Lunel F. Hepatitis C virus genotypes and subtypes in patients with hepatitis C, with and without cryoglobulinemia. J Hepatol 1996;25:427–432.
17. Fried MW, Buti M, Dore GJ, *et al.* Once-daily simeprevir (TMC435) with Pegylated interferon and ribavirin in treatment-naïve genotype 1 hepatitis C: the randomized PILLAR Study. Hepatology 2013;58:1918–1929.
18. Harwood NE, and Batista FD. New insights into the early molecular events underlying B cell activation. Immunity 2008;28:609–619.
19. Hsu M, Zhang J, Flint M, *et al.* Hepatitis C virus glycoproteins mediate pH-dependent cell entry of pseudotyped retroviral particles. Proc Natl Acad Sci U S A 2003;100: 7271–7276.
20. Inokuchi M, Ito T, Uchikoshi M, *et al.* Infection of B cells with hepatitis C virus for the development of lymphoproliferative disorders in patients with chronic hepatitis C. J Med Virol 2009;627:619–627.
21. Ito M, Masumi A, Mochida K, *et al.* Peripheral B cells may serve as a reservoir for persistent hepatitis C virus infection. J Innate Immun 2010;2:607–617.
22. Jacobson IM, McHutchison JG, Dusheiko G, *et al.* Telaprevir for previously untreated chronic hepatitis C virus infection. N Engl J Med 2011;364:2405–2416.
23. Jahan S, Khaliq S, Siddiqi MH, *et al.* Anti-apoptotic effect of HCV core gene of genotype 3a in Huh-7 cell line. Virol J 2011;8:522.
24. Kambara H, Fukuhara T, Shiokawa M, *et al.* Establishment of a novel permissive cell line for the propagation of hepatitis C virus by expression of microRNA miR122. J Virol 2012;86:1382–1393.
25. Karavattathayyil SJ, Kalkeri G, Liu HJ, *et al.* Detection of hepatitis C virus RNA sequences in B-cell non-Hodgkin lymphoma. Am J Clin Pathol 2000;113:391–398.
26. Kasama Y, Sekiguchi S, Saito M, *et al.* Persistent expression of the full genome of hepatitis C virus in B cells induces spontaneous development of B-cell lymphomas *in vivo*. Blood 2010;116;4926–4933.
27. Kondo Y, and Shimosegawa T. Direct effects of hepatitis C virus on the lymphoid cells. World J Gastroenterol 2013; 19:7889–7895.
28. Ladu S, Calvisi DF, Conner EA, Farina M, Factor VM, and Thorgeirsson SS. E2F1 inhibits c-Myc-driven apoptosis via PIK3CA/Akt/mTOR and COX-2 in a mouse model of human liver cancer. Gastroenterology 2008;135:1322–1332.
29. Lanford RE, Chavez D, Chisari FV, and Sureau C. Lack of detection of negative-strand hepatitis C virus RNA in peripheral blood mononuclear cells and other extrahepatic tissues by the highly strand-specific rTth reverse transcriptase PCR. J Virol 1995;69:8079–8083.
30. Laskus T, Radkowski M, Wang LF, Vargas H, and Rakela J. The presence of active hepatitis C virus replication in lymphoid tissue in patients coinfected with human immunodeficiency virus type 1. J Infect Dis 1998;178:1189–1192.
31. Lerat H, Berby F, Trabaud MA, *et al.* Specific detection of hepatitis C virus minus strand RNA in hematopoietic cells. J Clin Invest 1996;97:845–851.
32. Lok AS, Gardiner DF, Hézode C, *et al.* Randomized trial of daclatasvir and asunaprevir with or without PegIFN/RBV for hepatitis C virus genotype 1 null responders. J Hepatrol 2014;60:490–499.
33. Lowe SW, and Lin AW. Apoptosis in cancer. Carcinogenesis 2000;21:485–495.
34. MacParland SA, Pham TN, Guy CS, and Michalak TI. Hepatitis C virus persisting after clinically apparent sustained virological response to antiviral therapy retains infectivity *in vitro*. Hepatology 2009;49:1431–1441.
35. Marukian S, Jones CT, Andrus L, *et al.* Cell culture-produced hepatitis C virus does not infect peripheral blood mononuclear cells. Hepatology 2008;48:1843–1850.
36. Mazzaro C, Franzin F, Tulissi P, *et al.* Regression of monoclonal B-cell expansion in patients affected by mixed cryoglobulinemia responsive to alpha-interferon therapy. Cancer 1996;77:2604–2613.

37. McKeating JA, Zhang LQ, Logvinoff C, *et al.* Diverse hepatitis C virus glycoproteins mediate viral infection in a CD81-dependent manner. J Virol 2004;78:8496–8505.
38. Mizuochi T, Ito M, Takai K, and Yamaguchi K. Peripheral blood memory B cells are resistant to apoptosis in chronic hepatitis C patients. Virus Res 2011;155:349–351.
39. Murakami K, Kimura T, Shoji I, *et al.* Virological characterization of the hepatitis C virus JFH-1 strain in lymphocytic cell lines. J Gen Virol 2008;89:1587–1592.
40. Muratori L, Gibellini D, Lenzi M, *et al.* Quantification of hepatitis C virus-infected peripheral blood mononuclear cells by *in situ* reverse transcriptase-polymerase chain reaction. Blood 1996;88:2768–2774.
41. Phan T, Beran RKF, Peters C, Lorenz IC, and Lindenbach BD. Hepatitis C virus NS2 protein contributes to virus particle assembly via opposing epistatic interactions with the E1-E2 glycoprotein and NS3-NS4A enzyme complexes. J Virol 2009;83:8379–8395.
42. Pileri P, Uematsu Y, Campagnoli S, *et al.* Binding of hepatitis C virus to CD81. Science 1998;282:938–941.
43. Ploss A, Evans MJ, Gaysinskaya VA, *et al.* Human occludin is a hepatitis C virus entry factor required for infection of mouse cells. Nature 2009;457:882–886.
44. Qu J, Zhang Q, Li Y, *et al.* The Tat protein of human immunodeficiency virus-1 enhances hepatitis C virus replication through interferon gamma-inducible protein-10. BMC Immunol 2012;13:15.
45. Radkowski M, Gallegos-Orozco JF, Jablonska J, *et al.* Persistence of hepatitis C virus in patients successfully treated for chronic hepatitis C. Hepatology 2005;41:106–114.
46. Ramakrishnaiah V, Thumann C, Fofana I, *et al.* Exosome-mediated transmission of hepatitis C virus between human hepatoma Huh7.5 cells. Proc Natl Acad Sci U S A 2013; 110:13109–13113.
47. Sarhan MA, Pham TNQ, Chen AY, and Michalak TI. Hepatitis C virus infection of human T lymphocytes is mediated by CD5. J Virol 2012;86:3723–3735.
48. Schmidt WN, Stapleton JT, LaBrecque DR, *et al.* Hepatitis C virus (HCV) infection and cryoglobulinemia: analysis of whole blood and plasma HCV RNA concentrations and correlation with liver histology. Hepatology 2000;31: 737–744.
49. Schulze-Bergkamen H, Krammer P.H. Apoptosis in cancer—implications for therapy. Semin Oncol 2004;31: 90–119.
50. Seto WK, Lai CL, Fung J, *et al.* Natural history of chronic hepatitis C: genotype 1 versus genotype 6. J Hepatol 2010; 53:444–448.
51. Sung VM, Shimodaira S, Doughty AL, *et al.* Establishment of B-cell lymphoma cell lines persistently infected with hepatitis C virus *in vivo* and *in vitro*: the apoptotic effects of virus infection. J Virol 2003;77:2134–2146.
52. Turner NC. Hepatitis C and B-cell lymphoma. Ann Oncol 2003;14:1341–1345.
53. Wakita T, Pietschmann T, Kato T, *et al.* Production of infectious hepatitis C virus in tissue culture from a cloned viral genome. Nature Med 2005;11:791–796.

Address correspondence to:
Dr. Tsukasa Seya
Department of Microbiology and Immunology
Hokkaido University Graduate School of Medicine
Kita 15, Nishi 7
Kita-ku
Sapporo 060-8638
Japan

E-mail: seya-tu@pop.med.hokudai.ac.jp

Immunogenetics (2014) 66:161–170
DOI 10.1007/s00251-014-0760-y

ORIGINAL PAPER

Divergence and diversity of *ULBP2* genes in rhesus and cynomolgus macaques

Taeko K. Naruse · Hirofumi Akari · Tetsuro Matano · Akinori Kimura

Received: 10 November 2013 / Accepted: 13 January 2014 / Published online: 28 January 2014

Abstract Non-human primates such as rhesus macaque and cynomolgus macaque are important animals for medical research fields and they are classified as Old World monkey, in which genome structure is characterized by gene duplications. In the present study, we investigated polymorphisms in two genes for ULBP2 molecules that are ligands for NKG2D. A total of 15 and 11 *ULBP2.1* alleles and 11 and 10 *ULBP2.2* alleles were identified in rhesus macaques and cynomolgus macaques, respectively. Nucleotide sequences of exons for extra cellular domain were highly polymorphic and more than 70 % were non-synonymous variations in both *ULBP2.1* and *ULBP2.2*. In addition, phylogenetic analyses revealed that the *ULBP2.2* was diverged from a branch of *ULBP2.1* along with *ULBP2*s of higher primates. Moreover, when 3D structural models were constructed for the rhesus ULBP2 molecules, residues at presumed contact sites with NKG2D were polymorphic in *ULBP2.1* and *ULBP2.2* in the rhesus macaque and cynomolgus macaque, respectively. These observations suggest that amino acid replacements at the interaction sites with NKG2D might shape a specific nature of ULBP2 molecules in the Old World monkeys.

Keywords Rhesus macaque · Cynomolgus macaque · *ULBP2/RAET1H* · NKG2D · Polymorphisms

Electronic supplementary material The online version of this article (doi:10.1007/s00251-014-0760-y) contains supplementary material, which is available to authorized users.

T. K. Naruse · A. Kimura (✉)
Department of Molecular Pathogenesis, Medical Research Institute, Tokyo Medical and Dental University (TMDU), 1-5-45 Yushima, Bunkyo-ku, Tokyo 113-8510, Japan
e-mail: akitis@mri.tmd.ac.jp

H. Akari
Primate Research Institute, Kyoto University, Inuyama, Japan

T. Matano
AIDS Research Center, National Institute of Infectious Diseases, Tokyo, Japan

T. Matano
The Institute of Medical Science, The University of Tokyo, Tokyo, Japan

Introduction

Natural-killer group 2 member D (NKG2D), a C-type lectin molecule, is an activating receptor expressing on the surface of NK, $\gamma\delta^+$ and $CD8^+$ T cells, which plays an important role in the immune system (Wu et al., 1999; Raulet 2003). In humans, several MHC class I-like molecules are known as ligands for NKG2D, including MHC class I chain-related (MIC) and UL-16 binding protein (ULBP)/retinoic acid early transcript 1 (RAET1) (Bauer et al. 1999; Cosman et al. 2001; Chalupny et al. 2003; Bacon et al. 2004). These ligands are usually stress-inducible, and their recognition by NKG2D leads to the activation of NK cells, resulting in the killing of virus-infected cells and tumor cells (Pende et al. 2002; Eagle et al. 2006, Pappworth et al. 2007; Ward et al. 2007).

The human ULBP/RAET1 molecules are encoded by the *ULBP/RAET1* gene family located on the 6q24.2, which is composed of 10 members including six functional genes, *ULBP1*, *2*, *3*, *4*, *5*, and *6*, corresponding to *RAET1I*, *H*, *N*, *E*, *G*, and *L*, respectively (Radosavljevic et al. 2001; Chalupny et al. 2003; Eagle et al. 2009a, b; Eagle et al. 2009b). In addition, several sequence variations in each *ULBP* have been identified (Romphruk et al. 2009; Antoun et al. 2010). Although it is evident that the cell surface expression of the ligand molecules on target cells is differentially regulated (Eagle et al. 2006), genetic variations or polymorphisms in the coding region might also have a functional impact.

In the medical field, non-human primates including rhesus and cynomolgus macaques are used as animal models in the

immunological studies for infectious diseases, autoimmune diseases, organ transplantation, and development of vaccines. These macaques are members of the Old World monkey and it has been reported that the genetic diversity in the rhesus macaque is quite unique, i.e., more than 60 % of the rhesus macaque-specific expansions are found in the protein coding sequences (Gibbs et al. 2007). To fully evaluate the results of immunological experiments using macaque models, it is essential to characterize the genetic diversity of immune-related molecules, which may shape the basis of individual differences in the immune response against foreign antigens and/or pathogens. It has been reported that the copy numbers of genes in the major histocompatibility complex (MHC) loci in the Old World monkey are higher than those in humans (Kulski et al. 2004; Gibbs et al. 2007; Otting et al. 2007). In addition, the extent of genetic diversity in MHC differed, in part, depending on the geographic area, and we have reported that the diversity of MHC class I genes in the rhesus and cynomolgus macaques is considerably different depending on habitat (Naruse et al. 2010, Saito et al. 2012). In our previous study, we have demonstrated that *ULBP4* is more polymorphic in the Old World monkey than in humans (Naruse et al. 2011). It also was revealed that each member of the *ULBP/RAET1* gene family, except for *ULBP6*, had been duplicated in the rhesus genome (Naruse et al. 2011).

Recent reports have indicated that the expression of *ULBP2* is upregulated in HIV infection (Richard et al. 2013, Matusali et al. 2013). Because the innate immune system may be involved in the response to environmental pathogens, it is important to investigate the polymorphisms in the ligands of NK receptors in the experimental animal models for developing HIV vaccine. Here, we report the *ULBP2* polymorphisms focusing on the divergence and diversity in the Old World monkey.

Materials and methods

Animals

A total of 37 rhesus macaques and 24 cynomolgus macaques, previously analyzed for the polymorphisms in MHC class I genes (Naruse et al. 2010, Saito et al. 2012) were the subjects. They were maintained in the breeding colonies in Japan. The founders of the rhesus macaque colonies were captured in Myanmar and Laos, whereas the founders of cynomolgus macaque colonies were captured in Indonesia, Malaysia, and the Philippines. All care including blood sampling of animals were in accordance with the guidelines for the Care and Use of Laboratory Animals published by the National Institutes of Health (NIH publication 85-23, revised 1985) and the study protocol was subjected to prior approval by the local animal protection authority.

DNA extraction and sequencing analysis

Genomic DNAs of B lymphoblastoid cell lines from rhesus macaques and whole blood samples of cynomolgus macaques were prepared, as previously reported (Naruse et al. 2010, Saito et al. 2012). Amplification of *ULBP2* from macaques was done by polymerase chain reaction (PCR) with specific primer pairs designed for the region spanning from intron 1 to intron 3 of rhesus *ULBP2*, LOC694466 (designated as *ULBP2.1*) and LOC694600 (designated as *ULBP2.2*), using FastStart Taq DNA polymerase (Roche, Mannheim, Germany). Primer sequences are as follows: UL2.1NF (5′-AGGGGCTAACTAGGGGTCTTTC) and UL2.1NR (5′ ACCGTTTCTGATCTCATTCCA) for *ULBP2.1*, and UL2.2NF (5′-GAGGGCTAACTAGGGGTCTCT) and UL2.2NR (5′-ACCATTTCTGATCTCATTCCAGA) for *ULBP2.2*. The PCR program was composed of following steps: denaturation at 95 °C for 4 min; 30 cycles of 95 °C for 30 s, 56 °C for 30 s, 72 °C for 45 s; and additional extension at 72 °C for 7 min. The PCR products, about 1,400 bp for *ULBP2.1* and about 1,080 bp for *ULBP2.2*, were cloned into pSTBlue-1 AccepTer vector (Novagen, WI, USA) according to the manufacturer's instructions and transformed into Nova Blue Single™ competent cells (Merck Biosciences Japan, Tokyo, Japan). Ten to 20 independent transformed colonies were picked up for each sample and subjected to sequencing on both strands by using a BigDye Terminator cycling system and an ABI 3730 automated sequence analyzer (Applied Biosystems, CA, USA).

Data analysis

Nucleotide sequences from cloned DNAs were aligned using the Genetyx software package (version 8.0, Genetyx Corp., Japan). When at least three clones from independent PCR or from different subjects showed identical sequences, the sequences were submitted to the DNA Data Bank of Japan (DDBJ). A neighbor-joining tree was constructed by Kimura's two-parameter method for a phylogenetic analysis of *ULBP2* sequences from exon 2 to exon 3, excluding intron 2 sequences, by using the Genetyx software. Bootstrap values were based on 5,000 replications. The *ULBP2* and *ULBP6* sequences from human (GenBank accession numbers AL583835 and AL355497, respectively), and *ULBP2* sequences from chimpanzee (NC006473), western gorilla (NC018430), rhesus (NC007861), and another member of Old World monkey, olive baboon (NC018155) were included in the phylogenetic analysis. The *ULBP1* (LOC694341), *ULBP3* (LOC694525), *ULBP4* (LOC695031), and *ULBP5* (LOC694265) sequences from rhesus macaque, and *ULBP1* (NM025218), *ULBP3* (AL355497), *ULBP4* (AL355312), and *ULBP5* (AL583835) sequences from human were also included in the analysis.